USGS
science for a changing world

North Carolina Floodplain Mapping Program

LiDAR-Derived Flood-Inundation Maps for Real-Time Flood-Mapping Applications, Tar River Basin, North Carolina

Scientific Investigations Report 2007–5032

U.S. Department of the Interior
U.S. Geological Survey

Cover. Flooded subdivision in the Tar River basin, Greenville, North Carolina, October 1999 *(photograph was contributed by the Federal Emergency Management Agency)*.

LiDAR-Derived Flood-Inundation Maps for Real-Time Flood-Mapping Applications, Tar River Basin, North Carolina

By Jerad D. Bales, Chad R. Wagner, Kirsten C. Tighe, and Silvia Terziotti

North Carolina Floodplain Mapping Program

Scientific Investigations Report 2007–5032

U.S. Department of the Interior
U.S. Geological Survey

U.S. Department of the Interior
DIRK KEMPTHORNE, Secretary

U.S. Geological Survey
Mark D. Myers, Director

U.S. Geological Survey, Reston, Virginia: 2007

For product and ordering information:
World Wide Web: http://www.usgs.gov/pubprod
Telephone: 1-888-ASK-USGS

For more information on the USGS—the Federal source for science about the Earth, its natural and living resources, natural hazards, and the environment:
World Wide Web: http://www.usgs.gov
Telephone: 1-888-ASK-USGS

Suggested citation:
Bales, J.D., Wagner, C.R., Tighe, K.C., and Terziotti, Silvia, 2007, LiDAR-derived flood-inundation maps for real-time flood-mapping applications, Tar River basin, North Carolina: U.S. Geological Survey Scientific Investigations Report 2007–5032, 42 p.

Contents

Figures

Tables

Conversion Factors

SI to Inch/Pound

Multiply	By	To obtain
	Length	
centimeter (cm)	0.3937	inch (in.)
millimeter (mm)	0.03937	inch (in.)
meter (m)	3.281	foot (ft)
kilometer (km)	0.6214	mile (mi)
	Area	
square meter (m^2)	10.76	square foot (ft^2)
square kilometer (km^2)	0.3861	square mile (mi^2)
	Volume	
cubic meter (m^3)	264.2	gallon (gal)
cubic meter (m^3)	0.0002642	million gallons (Mgal)
cubic hectometer (hm^3)	810.7	acre-foot (acre-ft)
	Flow rate	
cubic meter per second (m^3/s)	35.31	cubic foot per second (ft^3/s)
cubic meter per day (m^3/d)	35.31	cubic foot per day (ft^3/d)
cubic meter per second (m^3/s)	22.83	million gallons per day (Mgal/d)
	Hydraulic gradient	
meter per kilometer (m/km)	5.27983	foot per mile (ft/mi)

Vertical coordinate information is referenced to the National American Vertical Datum of 1988 (NAVD 88).

Horizontal coordinate information (latitude and longitude) is referenced to the North American Datum of 1983 (NAD 83).

Altitude, as used in this report, refers to distance above the vertical datum.

Acronyms used in this report:

AVHRR	advanced very high resolution radiometer
DEM	digital elevation model
DFIRM	Digital Flood Insurance Rate Map
DGPS	differential global positioning system
FEMA	Federal Emergency Management Agency
FMP	Floodplain Mapping Program
GIS	geographic information system
HEC–RAS	Hydraulic Engineering Center–River Analysis System
HU	hydrologic unit
LiDAR	light detection and ranging
NCCGIA	North Carolina Center for Geographic Information and Analysis
NCDEM	North Carolina Division of Emergency Management
NCGS	North Carolina Geodetic Survey
NWS	National Weather Service
QC	quality control
SAR	synthetic aperture radar
TIN	triangulated irregular network
USGS	U.S. Geological Survey

North Carolina Floodplain Mapping Program

LiDAR-Derived Flood-Inundation Maps for Real-Time Flood-Mapping Applications, Tar River Basin, North Carolina

By Jerad D. Bales, Chad R. Wagner, Kirsten C. Tighe, and Silvia Terziotti

Abstract

Flood-inundation maps were created for selected streamgage sites in the North Carolina Tar River basin. Light detection and ranging (LiDAR) data with a vertical accuracy of about 20 centimeters, provided by the Floodplain Mapping Information System of the North Carolina Floodplain Mapping Program, were processed to produce topographic data for the inundation maps. Bare-earth mass point LiDAR data were reprocessed into a digital elevation model with regularly spaced 1.5-meter by 1.5-meter cells. A tool was developed as part of this project to connect flow paths, or streams, that were inappropriately disconnected in the digital elevation model by such features as a bridge or road crossing.

The Hydraulic Engineering Center–River Analysis System (HEC–RAS) model, developed by the U.S. Army Corps of Engineers, was used for hydraulic modeling at each of the study sites. Eleven individual hydraulic models were developed for the Tar River basin sites. Seven models were developed for reaches with a single gage, and four models were developed for reaches of the Tar River main stem that receive flow from major gaged tributaries, or reaches in which multiple gages were near one another. Combined, the Tar River hydraulic models included 272 kilometers of streams in the basin, including about 162 kilometers on the Tar River main stem.

The hydraulic models were calibrated to the most current stage-discharge relations at 11 long-term streamgages where rating curves were available. Medium- to high-flow discharge measurements were made at some of the sites without rating curves, and high-water marks from Hurricanes Fran and Floyd were available for high-stage calibration. Simulated rating curves matched measured curves over the full range of flows. Differences between measured and simulated water levels for a specified flow were no more than 0.44 meter and typically were less.

The calibrated models were used to generate a set of water-surface profiles for each of the 11 modeled reaches at 0.305-meter increments for water levels ranging from bankfull to approximately the highest recorded water level at the downstream-most gage in each modeled reach. Inundated areas were identified by subtracting the water-surface elevation in each 1.5-meter by 1.5-meter grid cell from the land-surface elevation in the cell through an automated routine that was developed to identify all inundated cells hydraulically connected to the cell at the downstream-most gage in the model domain.

Inundation maps showing transportation networks and orthoimagery were prepared for display on the Internet. These maps also are linked to the U.S. Geological Survey North Carolina Water Science Center real-time streamflow website. Hence, a user can determine the near real-time stage and water-surface elevation at a U.S. Geological Survey streamgage site in the Tar River basin and link directly to the flood-inundation maps for a depiction of the estimated inundated area at the current water level.

Although the flood-inundation maps represent distinct boundaries of inundated areas, some uncertainties are associated with these maps. These are uncertainties in the topographic data for the hydraulic model computational grid and inundation maps, effective friction values (Manning's n), model-validation data, and forecast hydrographs, if used.

The Tar River flood-inundation maps were developed by using a steady-flow hydraulic model. This assumption clearly has less of an effect on inundation maps produced for low flows than for high flows when it typically takes more time to inundate areas. A flood in which water levels peak and fall slowly most likely will result in more inundation than a similar flood in which water levels peak and fall quickly. Limitations associated with the steady-flow assumption for hydraulic modeling vary from site to site.

The one-dimensional modeling approach used in this study resulted in good agreement between measurements and

simulations. The one-dimensional approach is reasonable for a prismatic channel in a relatively narrow floodplain but may not be appropriate for sinuous rivers with several tributaries in broad floodplains. Uncertainty in the flood-inundation polygons increases with distance from the main channel for which water-surface slopes are simulated. Two-dimensional models are increasingly used for simulating floodplain inundation because of the variability in topography across the floodplain, particularly in wide floodplains with numerous tributaries.

Introduction

Floods affect all parts of North Carolina. Of the 50 states, North Carolina had the ninth highest total flood damages (measured in 1995 dollars) during 1983–2003, and the twelfth highest damages per capita (Pielke and others, 2002; University Corporation for Atmospheric Research, 2006).

A few major floods in North Carolina have been associated with stalled frontal systems, such as the widespread and damaging flood that occurred in a 16-county area of western North Carolina in November 1977 (Zembrzuski and others, 1991). Most North Carolina floods with exceedance levels in excess of about 10 years, however, typically result from relatively short-duration, locally intense rainfall or from rainfall associated with tropical cyclones. Flash floods from locally intense rainfall most commonly occur in the Blue Ridge Physiographic Province and in large urban areas across the State (for example, Mason and Caldwell, 1993; Eddins and Zembrzuski, 1998; Robinson and others, 1998).

Tropical cyclones and the remnants of tropical cyclones have caused flooding in all parts of North Carolina (Zembrzuski and others, 1991). Tropical cyclones generated devastating floods in the Blue Ridge Physiographic Province in 1916, 1928, 1940, and most recently in 2004. Within a period of less than 2 weeks in September 2004, Hurricanes Frances and Ivan produced back-to-back floods having exceedance levels of 100 years or greater (U.S. Geological Survey, 2006d). Maximum water levels established during the 1940 flood were exceeded in many locations during 2004, although maximum water levels established along parts of the French Broad River during the 1916 flood were not exceeded in 2004. The Pigeon River basin was affected particularly by the storms; flood peaks at Canton for both Frances and Ivan were at the 500-year exceedance level (based on an analysis of flood peaks through 1996; Pope and others, 2001).

Widespread and destructive floods produced by rainfall from tropical cyclones also can occur in the Piedmont and Coastal Plain of North Carolina. The 1916 and 1940 floods occurred not only in the Blue Ridge but also extended into the Piedmont Physiographic Province. Because of the remnants of a tropical cyclone that traveled from extreme northwestern North Carolina into the Sand Hills and on into the extreme northeastern part of North Carolina, the 1940 flood included the Coastal Plain as well (Zembrzuski and others, 1991). Tropical cyclones in 1954 and 1955 also produced widespread flooding in the Coastal Plain and, to a lesser extent, the Piedmont, but tropical cyclones produced relatively little regional flooding in these provinces between 1956 and 1995 when tropical cyclone activity was somewhat low (Bales and others, 2000). A period of more intense tropical cyclone activity began in 1996 and continued through at least 2005. Hurricane Fran in 1996 produced fairly widespread flooding in the Neuse, Tar, and Cape Fear River basins (Bales and Childress, 1996), with floods at the 100-year exceedance level in several locations.

Flooding from Hurricanes Dennis and Floyd in 1999 was among the most destructive and widespread in North Carolina in the last 100 years (Bales and others, 2000). Flooding at the 500-year exceedance level occurred in all of the major river basins draining to Pamlico Sound (Bales, 2003), and 66 of the 100 North Carolina counties were declared disaster areas. Damages from Hurricane Floyd were estimated to be in excess of $3.5 billion, including the destruction of more than 4,100 uninsured or underinsured homes (North Carolina Floodplain Mapping Program, 2006).

Flooding from Hurricanes Fran, Dennis, Floyd, Frances, and Ivan clearly demonstrated a growing demand and need for more and better flood information and flood forecasts. Flood-information products are needed that (1) are available for more locations, (2) provide mapped information on inundated areas rather than on river stage only, and (3) interface with a full suite of other flood-related products, such as Digital Flood Insurance Rate Maps (DFIRMs) and flood-forecast products produced by the National Weather Service (NWS). Such information must be readily available for both governmental officials and the citizens of North Carolina in an easily understood format.

Based on experiences from Hurricane Floyd flooding, the Governor of North Carolina and the North Carolina General Assembly assigned the North Carolina Floodplain Mapping Program (FMP) in 2000 the task of improving flood information and flood forecasting in the State. The primary goal of the long-term effort is to provide emergency managers and the public with more accessible, informative, timely, and accurate flood information and flood-forecast products for more locations. The FMP, which is in the Office of Geospatial and Technology Management in the North Carolina Division of Emergency Management (NCDEM), is working cooperatively with other offices in NCDEM, the North Carolina Center for Geographic Information and Analysis (NCCGIA), other State and local agencies, the NWS, the Federal Emergency Management Agency (FEMA), and the U.S. Geological Survey (USGS) to develop and demonstrate technology to improve flood forecasts and information dissemination.

One of the primary roles of the USGS in this multiagency effort is to develop and demonstrate the technology for producing detailed flood-inundation maps. These maps can be used in conjunction with USGS real-time streamgage data and a flood-inundation mapping and alert network being developed

by the FMP and NCCGIA to depict current areas of inundation and to provide estimates of areas that are expected, based on NWS flood forecasts, to become inundated hours or even days into the future. The maps also can be used separately as stand-alone products to provide emergency managers and the public with detailed estimates of flood inundation over a range of river stages.

Purpose and Scope

The purpose of this report is to document methods of the USGS, in cooperation with the North Carolina Floodplain Mapping Program, to create flood-inundation maps. Maps of selected streamgage sites in the Tar River basin, North Carolina (fig. 1), were created to demonstrate flood-inundation mapping technology. Maps were produced for water levels ranging from approximately bankfull to the maximum observed water level at each site. The hydrologic and topographic data used to create the maps are described herein, as are the methods for processing raw topographic data. Hydraulic modeling methods and results are described, and uncertainties associated with the inundation maps are discussed. An example of the metadata for one set of inundation maps is provided in Appendix 1.

Study Area

The Tar-Pamlico River basin is one of four major river basins that are contained entirely within North Carolina. The basin, as identified by the State of North Carolina, includes five 8-digit hydrologic units (HUs; fig. 1). This study includes only the part of the basin upstream from Washington, or HUs

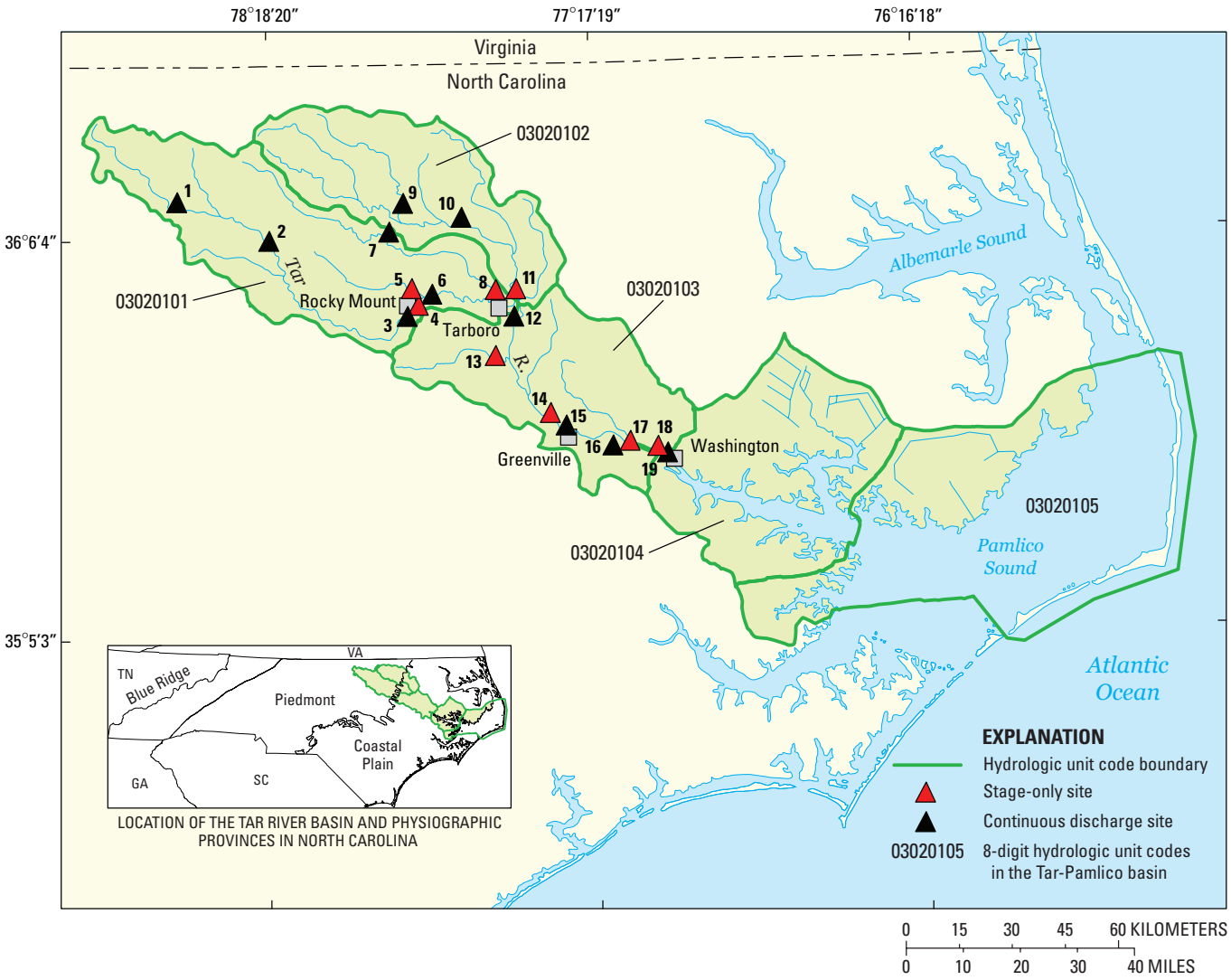

Figure 1. Selected study sites in the Tar-Pamlico River basin, North Carolina.

03020101, 03020102, and 03020103. The drainage area of the basin at Washington is about 8,300 square kilometers (km^2).

In 2000, the population of the basin was 393,217, a density of 48 people per square kilometer (people/km^2) in contrast to a statewide density of 59 people/km^2 (North Carolina Division of Water Quality, 2004). Major cities in the basin include Rocky Mount and Greenville. Population density in 2000 for HU 03020103, which includes the city of Greenville, was 68 people/km^2. Population in Greenville increased 8.4 percent between April 2000 and July 2003, nearly twice the population-growth rate for the entire State during the same period (U.S. Census Bureau, 2006a). Rocky Mount had essentially no population change during the same period (U.S. Census Bureau, 2006b). Population in the western part of the basin, which is within commuting distance of the Research Triangle (Raleigh-Durham-Chapel Hill area), is expected to increase by almost 50 percent between the years 2000 and 2020, and the population in the Greenville area is expected to grow about 40 percent during the same period (North Carolina Division of Water Quality, 2004).

About 7 percent of the land in the basin is classified as urban or developed. Almost two-thirds of the land cover in HU 03020102 is forest. The lowest percentage of forest land cover is in HU 03020103, which is entirely in the Coastal Plain; this HU also has the highest percentage of cropland (40 percent) in the basin (North Carolina Division of Water Quality, 2004). In March 2003, 13 registered poultry operations and 101 registered swine operations were located in the basin (North Carolina Division of Water Quality, 2004). Most of the poultry operations were in the western part of the basin, west of Rocky Mount. Swine operations were distributed relatively uniformly except in the extreme western part of the basin where no registered swine operations were located.

Average annual precipitation in the basin ranges from 115.6 centimeters (cm) at Oxford, in the western end of the basin, to 125.5 cm at Washington (State Climate Office of North Carolina, 2006). Highest monthly rainfall typically occurs during the summer, although the seasonal difference is greater in the eastern part of the basin than in the western part. Average annual evapotranspiration ranges from about 81 cm in the western part of the basin to about 86 cm in the eastern part (Mason and Jackson, 1986). Mean monthly streamflow is strongly seasonal, ranging from 33 cubic meters per second (m^3/s) in October to 125 m^3/s in March at Tar River at Tarboro (site 12, fig. 1), which is typical of other locations throughout the basin.

Streamflow data for the Tar River at Tarboro extends back to 1897 (fig. 2), and the period of record at this gage is among the longest in the Nation. The peak flow from Hurricane Floyd in 1999 was by far the greatest during more than 100 years

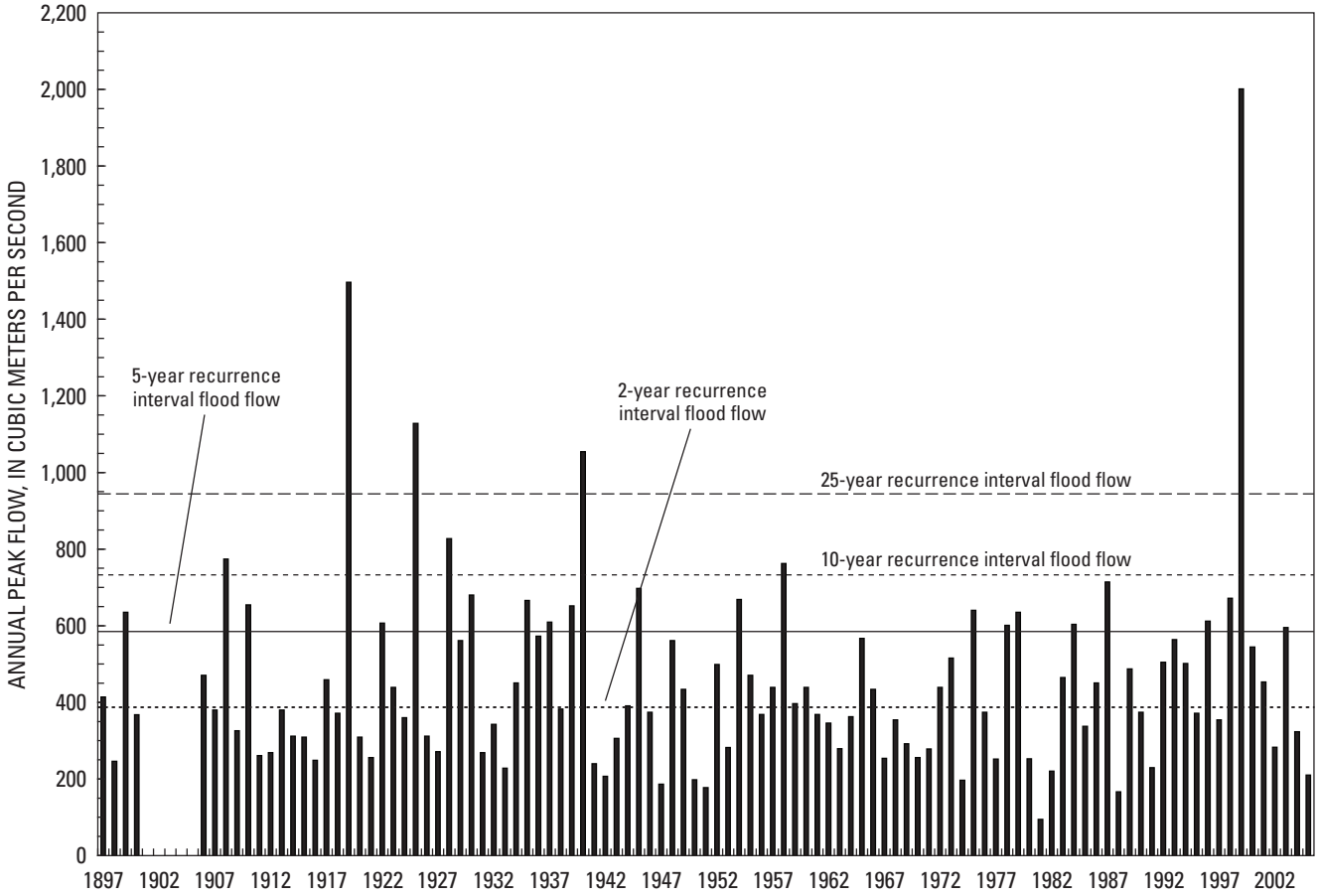

Figure 2. Annual flood peaks for the Tar River at Tarboro, North Carolina, 1897–2000 and 1906–2005.

of record (fig. 2). Other than the Hurricane Floyd flood, only one flood has been greater than the 10-year exceedance level since 1941 (fig. 2). During the 33-year period between 1908 and 1940, however, five floods were at the 10-year exceedance level or greater.

During 1960–2005, the highest annual peak flow (or annual flood) on the main stem Tar River at Tarboro (site 12, fig. 1) and on a tributary (site 9, fig. 1 (Little Fishing Creek near White Oak)) occurred in all months of the year except December (fig. 3). (The common period of record for the two gages is 1960–2005.) More than 55 percent of the annual floods at Tarboro, which has a drainage area of 5,653 km^2, occurred during the winter months of January–March, however, compared to 38 percent at Little Fishing Creek, which has a drainage area of 458 km^2 (table 1). During the summer months of June–August, 23 percent of the annual floods occurred at Little Fishing Creek compared to 9 percent at Tarboro. This is likely because the smaller basin is more readily affected by convective storms that occur in the summer.

All of the annual floods with an exceedance level greater than 10 years at the Tar River at Tarboro occurred during the months of May–October (fig. 4), although most of the annual floods occurred during the winter months (fig. 3). Of the 10 largest annual floods at Tarboro, 7 floods occurred during the months of July–October, and 4 occurred in September alone. All seven of these floods were associated with tropical cyclones, except perhaps for the 1919 flood (National Oceanic and Atmospheric Administration, 2006). Most of the annual floods at the 2- to 5-year exceedance levels, however, occurred during the winter.

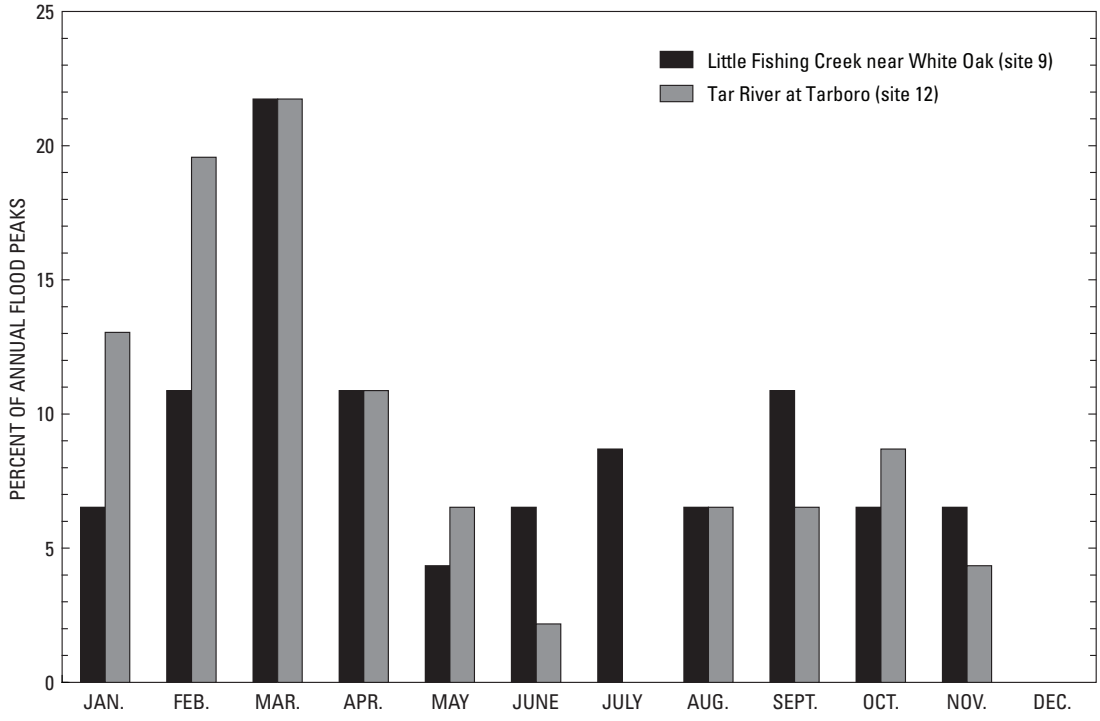

Figure 3. Annual flood peaks, in percent by month, for Tar River at Tarboro and Little Fishing Creek near White Oak, North Carolina, 1960–2005.

Table 1. Study sites in the Tar River basin of North Carolina.

[NAD 83, North American Datum of 1983; km^2, square kilometers; m, meter; NAVD 88, North American Vertical Datum of 1988; m^3/s, cubic meters per second; S, stage; Q, discharge; RF, precipitation; NA, not applicable; SR, secondary road; ND, not determined. Station numbers in **bold** type are National Weather Service Flood Forecast locations]

Site no. (fig. 1)	USGS station no.	Site name	County	Latitude (NAD 83)	Longitude (NAD 83)	Drainage area (km^2)	Data type	Beginning of record	Maximum recorded elevation at gage (m above NAVD 88) and date[a]	Maximum recorded streamflow at gage (m^3/s) and date[a]
1	02081500	Tar River near Tar River	Granville	36°11'39"	78°34'59"	432	S, Q	10/1939	94.63 (9/6/1996)	564.1 (9/6/1996)
2	**02081747**	Tar River at U.S. 401 at Louisburg	Franklin	36°05'35"	78°17'46"	1,105	S, Q, RF	10/1963	61.52 (9/17/1999)	671.8 (9/17/1999)
3	02082506	Tar River below Tar River Reservoir near Rocky Mount	Nash	35°54'02"	77°51'56"	2,012	S, Q	8/1972	35.90 (9/16/1999)	830.5 (9/16/1999)
4	0208250885	Tar River at U.S. 301 Bypass at Rocky Mount	Nash	35°55'34"	77°49'50"	2,038	S, RF	5/2003	27.79 (8/17/2004)	NA
5	02082576	Stony Creek at Winstead Avenue at Rocky Mount	Nash	35°58'06"	77°50'59"	290	S	7/2003	30.38 (9/1/2004)	NA
6	**02082585**	Tar River at NC 97 at Rocky Mount	Edgecombe	35°57'17"	77°47'14"	2,396	S, Q, RF	8/1976	25.75 (9/17/1999)	966.5 (9/17/1999)
7	02082770	Swift Creek at Hilliardston	Nash	36°06'44"	77°55'12"	430	S, Q	7/1963	45.95 (9/17/1999)	651.9 (9/17/1999)
8	0208281175	Swift Creek at NC 97 near Leggett	Edgecombe	35°58'49"	77°35'40"	681	S, RF	1/2003	15.08 (4/11,12/2003)	NA
9	02082950	Little Fishing Creek near White Oak	Halifax	36°11'00"	77°52'34"	458	S, Q	10/1959	44.58 (9/16/1999)	878.7 (9/16/1999)
10	**02083000**	Fishing Creek near Enfield	Edgecombe	36°09'02"	77°41'35"	1,362	S, Q	10/1923	28.93 (9/18/1999)	853.2 (9/18/1999)
11	0208331077	Fishing Creek at NC 97 near Leggett	Edgecombe	36°00'30"	77°31'33"	1,963	S	1/2003	14.93 (9/23/2003)	NA
12	**02083500**	Tar River at Tarboro	Edgecombe	35°53'40"	77°31'59"	5,653	S, Q	7/1896	15.50 (9/19/1999)	2,001 (9/19/1999)
13	02083640	Town Creek at U.S. 258 near Pinetops	Edgecombe	35°47'53"	77°35'29"	492	S, RF	7/2003	7.90 (9/20/2003)	NA
14	02083893	Tar River at U.S. 264 Bypass near Rock Springs	Pitt	35°38'43"	77°25'22"	6,788	S	6/2003	4.62 (8/20/2004)	NA
15	**02084000**	Tar River at Greenville	Pitt	35°37'00"	77°22'22"	6,889	S, Q, RF	5/1997	7.98 (9/21/1999)	2,069 (9/21/1999)
16	02084160	Chicod Creek at SR 1760 near Simpson	Pitt	35°33'42"	77°13'51"	116	S, Q	10/1975	6.21 (9/18/1999)	ND
17	02084173	Tar River at SR 1565 near Grimesland	Pitt	35°34'26"	77°10'33"	7,402	S	5/2003	1.26 (9/18/2003)	NA
18	0208436195	Tranters Creek at SR 1403 near Washington	Beaufort	35°33'47"	77°05'10"	637	S, RF	6/2003	1.52 (9/18/2003)	NA
19[b]	02084472[b]	Pamlico River at Washington	Beaufort	35°32'36"	77°03'43"	8,288	S, Q	10/1999	2.14 (9/21/1999)	2,353 (9/21/1999)

[a]Records through September 30, 2005.

[b]Flood-inundation maps were not created for this site.

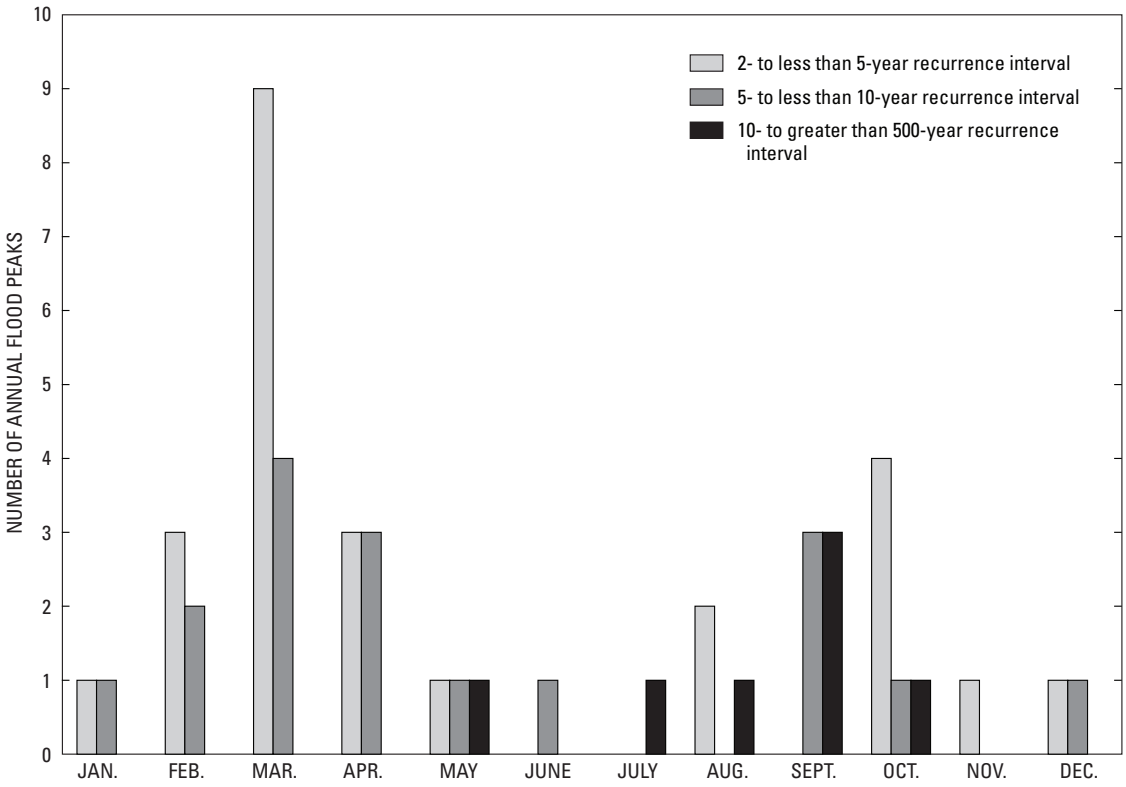

Figure 4. Annual flood peaks, by month, and recurrence intervals at the Tar River at Tarboro, North Carolina, 1897–1900 and 1906–2005.

Data

One of the keys for the development of reliable flood-inundation maps is the availability of detailed topographic data of known quality. The topographic data that were processed for hydraulic modeling and the creation of inundation maps are described here, as are the hydrologic data that were used in model calibration and testing.

Hydrologic Data

The Tar River basin hydrologic network consists of 19 streamgages (fig. 1; table 1). All of the gages are equipped with satellite radio transmitters that allow data to be accessed routinely on the Internet within an hour of collection and within about 15 minutes during floods. Five of the sites are NWS flood-forecast data sites (National Weather Service, 2006). Flood-inundation maps were created for 18 of these sites; the exception was the Pamlico River at Washington (site 19), where flooding can result from storm surge, upland flooding, or a combination of conditions.

Water level is measured continuously at all of the sites using methods described by Buchanan and Somers (1982) and Kennedy (1990). Continuous records of streamflow are computed at 11 of the 19 sites. Streamflow measurement and computation methods are documented by Rantz and others (1982), Morlock and others (2002), Simpson (2002), and Oberg and others (2005). Water-surface elevations are referenced to North American Vertical Datum of 1988 (NAVD 88).

Discrete discharge measurements were made at sites for which long-term streamflow records were unavailable (table 1). These measurements were made during periods of moderate to high flow and were used for model calibration. High-water marks measured following Hurricane Fran and Hurricane Floyd floods also were used as data for model calibration (U.S. Army Corps of Engineers, 1997; Federal Emergency Management Agency, 2000).

Topographic Data Derived from Light Detection and Ranging (LiDAR) Systems

The topographic-data source and quality-control (QC) measures performed on the data are discussed herein. Procedures used by the USGS to prepare the data for use in the hydraulic models and for development of inundation maps also are discussed.

Sources of LiDAR Data

The development of DFIRMS requires accurate land-surface elevation data. LiDAR systems were used to collect elevation data and the horizontal position of each elevation

data point for the Tar River basin during January–March 2001 (North Carolina Floodplain Mapping Program, 2003). Raw data subsequently were processed to remove LiDAR returns from such objects as trees, buildings, and other structures. The resulting product, called bare-earth mass points data, is available online from the FMP in 3,048-meter (m) by 3,048-m tiles (North Carolina Floodplain Mapping Program, 2003). Horizontal position is referenced to the North Carolina State Plane coordinate system, North American Datum of 1983 (NAD 83), and vertical position is referenced to NAVD 88.

Accuracy of Original LiDAR Data

The North Carolina Geodetic Survey (NCGS) collected QC information for the LiDAR bare-earth mass points data (North Carolina Geodetic Survey, 2002). Ground surveys were made by NCGS personnel for at least 100 points in each county in which LiDAR data were collected. Survey points were distributed among five different land-cover classes (grass, weeds or crops, scrub, forest, and developed), and the percentage of the survey points for each of the five land-cover classes was approximately proportional to the percentage of each land-cover class in the county. The percentage (5 percent) of the land-survey points that had the greatest error between the LiDAR data and land-survey positions were removed from the QC data set, and the statistics on the remaining points were computed (table 2). Statistics were computed both for the entire county and for the portion of the county within the Tar River basin; table 2 contains statistics for the part of each county that lies within the basin. The root mean square error (the difference between control-point elevations and LiDAR elevations) for all of the counties in the Tar River basin was less than 20 cm, which is the vertical accuracy required by the FMP for acceptance of LiDAR data measured in Coastal Plain counties. The vertical accuracy required for counties in the Piedmont is 25 cm.

The absolute maximum difference between LiDAR-derived land-surface elevations and ground-survey elevations was about 40 cm for the Tar River basin counties, although the absolute maximum difference in most counties was less than 30 cm. More than 50 percent of the LiDAR-derived elevations at the ground-control points were within 7 cm of the actual elevation for Tar River basin counties in which USGS streamgages are located (table 2). In general, LiDAR-derived elevations tended to be higher than actual land-surface elevations. Although no real pattern was obvious in the relation between land cover and the maximum error, the largest error was associated with scrub or forested lands, and the smallest error was associated with grass or developed land cover.

Conversion of LiDAR Data to Digital Elevation Model

Bare-earth mass point data received from the FMP were a collection of irregularly spaced points. These data were reprocessed into a digital elevation model (DEM) with regularly spaced, 1.5-m by 1.5-m cells. The DEM was created by first generating a triangulated irregular network (TIN). A TIN maintains the exact horizontal and vertical positions of the source data at the vertices of each triangle in the TIN, thus maintaining the integrity of the original data. Other horizontal and vertical positions can be interpolated along the edges and faces of the triangles in the TIN. A representation of major streams (known as break lines) provided by the FMP was used to guide the interpolation along the edges of the triangles. LiDAR-derived surfaces stored as 6.1-m by 6.1-m cell DEMs also are available from the FMP, although this resolution did not adequately capture the variations in topography that were needed to generate the flood-inundation maps at a resolution consistent with the resolution of the LiDAR data (for example, fig. 5).

The bare-earth mass points data were reprocessed to make use of all of the individual LiDAR points available. The TIN was interpolated to a finer resolution than FMP specifications require for production of DFIRMs to preserve as many original individual points as possible in the development of the DEM. This approach is similar in concept to using the TIN directly for elevation data; but because the TIN processes very slowly in a geographic information system (GIS) environment, a finer resolution DEM that is very nearly the same as the TIN but processes more quickly was created.

Table 2. LiDAR quality-control statistics for the Tar River basin, North Carolina (summarized from North Carolina Geodetic Survey, 2002).

[USGS, U.S. Geological Survey]

County[a]	Error statistics, in centimeters			Number of USGS streamgages, by county, in the Tar River basin
	Root mean square error	Mean error[b]	Median error[b]	
Edgecombe	17.4	-2.2	-3.8	6
Franklin	16.5	-6.1	-6.7	1
Granville	13.3	-1.4	-1.9	1
Halifax	14.7	6.9	6.5	1
Martin	14.4	-2.6	-1.3	0
Nash	14.2	1.2	0.8	4
Pitt	11.7	-4.6	-6.3	4
Vance	17.9	-6.3	-7.4	0
Warren	14.4	0.7	-0.6	0
Wilson	19.3	-13.7	-14.3	0

[a]Statistics for Beaufort County were unavailable.

[b]Negative values indicate that LiDAR values exceed ground-survey values.

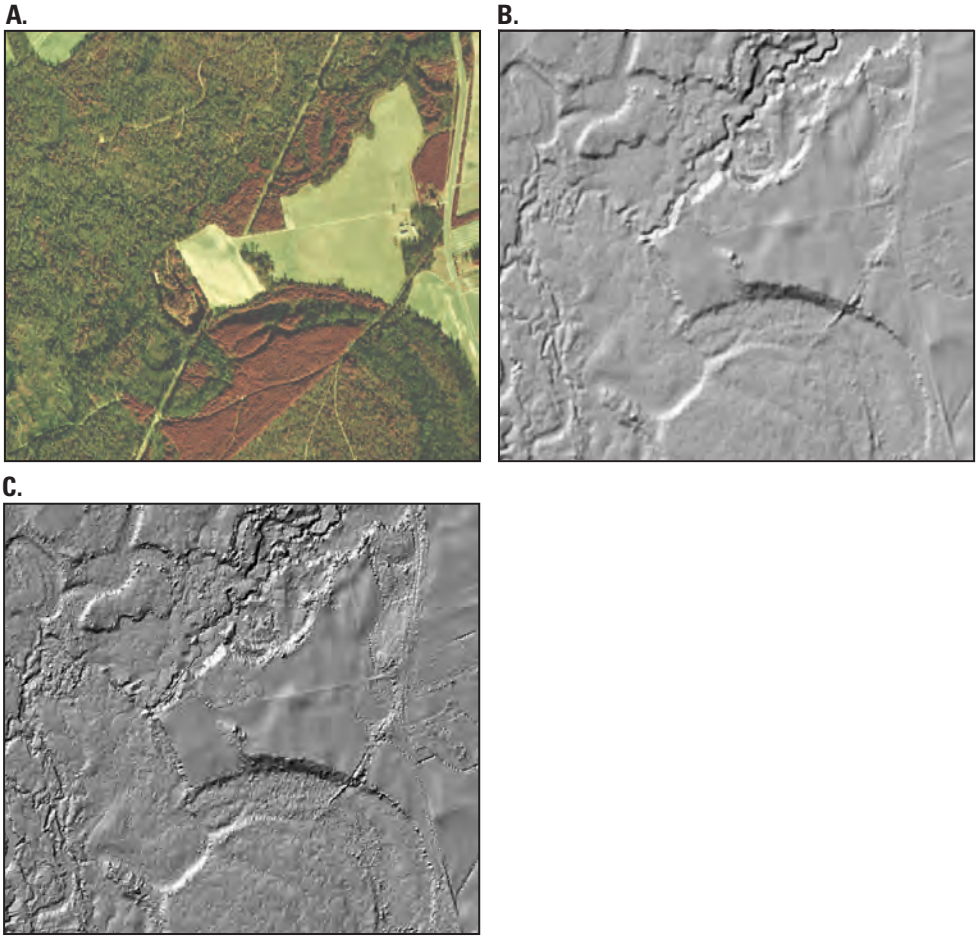

Figure 5. (A) Orthophotograph, (B) 6.1-meter by 6.1-meter digital elevation model, and (C) 1.5-meter by 1.5-meter digital elevation model of the Tar River floodplain near Tarboro in Edgecombe County, North Carolina. (A vertical exaggeration of 5 was applied to display the hillshade surfaces.)

Hydroconditioning of LiDAR Surfaces

The LiDAR return signal is based on the reflection of the laser from a solid surface. Hence, when a road crosses a stream, the LiDAR-derived DEM maintains the elevation of the road as the land-surface elevation, resulting in a discontinuous stream channel (fig. 6). The road as represented by the DEM becomes, in effect, a dam on the stream through which flow cannot pass. When calculating inundation areas from downstream to upstream locations, it is important for the flow path (stream channel) to be continuous along streambeds and low-lying areas. A tool, which is an ARC-Info script, was developed as part of this study to connect flow paths that were inappropriately disconnected by such features as bridges or road crossings. This tool uses the DEM, the road network, and the stream network to automatically (1) identify road and stream intersections, (2) identify the lowest elevation on the DEM within a specified distance (or buffer) on both sides of a road and stream intersection, (3) create a segment that connects these two low points, (4) assign this created segment the lowest elevation value within the buffer, and (5) integrate the segment back into the DEM so that a flow path is created through the road, connecting the upstream and downstream water segments (fig. 6). This then allows proper representation of inundated areas. This hydroconditioning process is not related to hydraulic modeling of flows through bridges or culverts, which is discussed later.

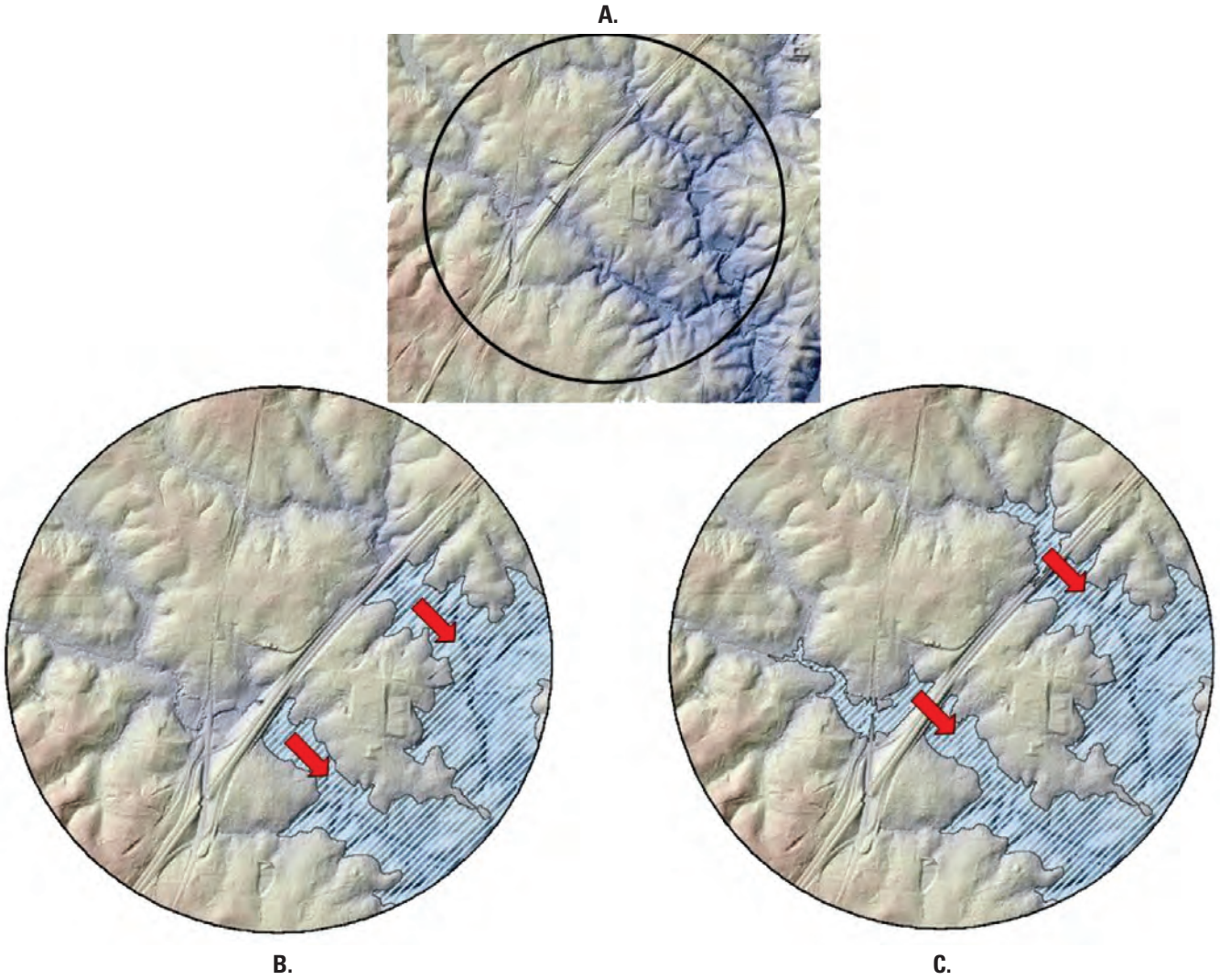

Figure 6. (A) Hill shade digital elevation model of the area near the confluence of Crisp Creek with Conetoe Creek in North Carolina, showing the inundated area (B) before and (C) after hydroconditioning. (Red arrows indicate direction of streamflow.)

Quality Assurance

Following reprocessing of the LiDAR data and hydroconditioning of the DEM, all elevation surfaces in areas that potentially could be inundated were carefully reviewed. Two steps were taken to identify potential problems with the DEM. First, the maximum and minimum elevations within each 3,048-m by 3,048-m tile were computed. If values were unexpectedly high or low, the tile was examined visually for problems (for example, fig. 7). Second, after inundation polygons were developed, all inundated areas were examined for the presence of islands and to ensure that hydroconditioning was complete. When islands were identified in the DEM, orthophotographs were examined to determine if the islands could be documented in the orthophotographs. Land-surface elevations that were in error and affected the inundation mapping results were smoothed by assigning an elevation value that was equal to that of surrounding points.

Figure 7. Example of spurious spike in the elevation surface.

Development of Flood-Inundation Maps

Flood-inundation maps were created for each of 18 streamgage sites in the Tar River basin by simulating the water-surface elevations along a stream reach that includes a streamgage and then combining this elevation with the topographic data to create a two-dimensional mapped water surface, or flood polygon. The hydraulic modeling for simulating the water-surface profiles is documented in this section, as is the approach used to create the flood polygons. Uncertainties associated with the approach and with the final results also are presented.

Hydraulic Modeling

The one-dimensional, step-backwater model, Hydraulic Engineering Center–River Analysis System (HEC–RAS), was used for hydraulic modeling at each of the study sites (Hydrologic Engineering Center, 2002). Version 3.1.3, released in May 2005 (Hydrologic Engineering Center, 2006), was used for this application. HEC–RAS is widely used for simulating steady-flow water-surface profiles in stream reaches and for one-dimensional hydraulic analysis at bridge crossings. The one-dimensional energy equation is solved within HEC–RAS for determination of water-surface profiles. The momentum equation can be included in the solution for situations in which the water-surface profile changes markedly with distance, such as at hydraulic jumps, bridges and culverts, and stream junctions. The effects of obstructions, such as bridges, culverts, weirs, and structures in the floodplain, are included in the hydraulic computations (Hydrologic Engineering Center, 2002). Unsteady-flow simulations also can be performed using HEC–RAS.

Eleven individual hydraulic models were developed for the Tar River basin sites (table 3). Seven models were developed for reaches with a single streamgage, and four models were developed for reaches of the Tar River main stem that receive flow from major gaged tributaries, or reaches in which multiple gages are near one another.

Table 3. Summary of hydraulic models developed for the Tar River basin study sites in North Carolina.

[m, meter; NAVD 88, North American Vertical Datum of 1988; MRC, measured stage-discharge rating curve; HWM, high-water mark; QM, measured discharge; —, no information available for calibration]

Model name	Streams in model	Site number (fig. 1)	Model reach length (m)	Number of cross sections in model	Average bed slope over reach	Number of bridges in reach	Range in Manning's *n* for reach	Range in simulated water-surface elevations at gage site (m above NAVD 88)	Model calibration method
Tar River	Tar River	1	10,660	33	0.00088	2	0.060 – 0.19	88.09 – 95.56	MRC
Louisburg	Tar River	2	9,145	31	0.00023	2	0.060 – 0.20	55.78 – 62.48	MRC
Rocky Mount	Tar River	3, 4, 6	19,777	43	0.00051	12	0.035 – 6.77	29.57 – 36.42[a]	MRC, HWM
	Stony Creek	5	9,405	77	0.00055	8	0.045 – 0.20	28.83 – 34.91	HWM, QM
Hilliardston	Swift Creek	7	10,644	41	0.00049	3	0.075 – 0.40	41.15 – 46.48	MRC
Little Fishing	Little Fishing Creek	9	11,278	40	0.00039	3	0.060 – 0.39	36.88 – 45.11	MRC
Enfield	Fishing Creek	10	13,564	35	0.00032	3	0.060 – 0.64	24.84 – 29.26	MRC
Tarboro	Swift Creek	8	11,674	28	0.00047	2	0.065 – 0.38	14.11 – 18.33	—
	Fishing Creek	11	18,471	39	0.00027	2	0.059 – 0.40	12.83 – 17.74	—
	Tar River	12	55,848	83	0.00018	7	0.030 – 1.00	8.38 – 16.00	MRC
Pinetops	Town Creek	13	18,322	41	0.00031	3	0.028 – 0.20	9.75 – 17.22	HWM, QM
Greenville	Tar River	14, 15	40,397	55	0.00011	6	0.055 – 6.05	2.64 – 8.83[b]	MRC, HWM
Grimesland	Chicod Creek	16	11,668	60	0.00071	3	0.058 – 2.96	1.27 – 6.22	MRC
	Tar River	17	13,863	30	0.00013	1	0.045 – 2.74	-0.31 – 5.79	HWM
Washington	Tranters Creek	18	11,887	24	-0.00016	1	0.047 – 0.35	-0.15 – 2.74	HWM, QM
	Tar River / Pamlico River	19	5,820	13	0.00037	1	0.041 – 0.40	-0.17 – 2.05	MRC

[a]Referenced to site 3. [b]Referenced to site 14.

Model domains were established so that model boundaries did not extend beyond any major changes in the stream relative to conditions at the gage. Inundation maps were not developed for the entire model domain for the Tarboro and Washington models because of uncertainties near model boundaries.

The FMP provided the USGS with selected HEC–RAS models that were constructed by contractors for the creation of DFIRMs. The FMP provided the Rocky Mount model, the Hilliardston model, the Enfield model, the Tarboro Tar River reach model, the Greenville model, and the Grimesland Tar River reach model (table 3). These models were tested by the USGS, and the models performed satisfactorily for flows in excess of approximately the 100-year exceedance level, or flows primarily used in the development of DFIRMs. The models generally did not perform adequately for development of flood-inundation maps at flows ranging from bankfull to about the 100-year flow. Hence, all of these models required additional development, calibration, and testing to simulate water levels with sufficient accuracy for inundation mapping.

Geometry Data

Bathymetric and topographic data used to develop the inundation models were derived from existing FMP models, LiDAR data, field surveys, and interpolation of measured information. The hydraulic models provided by the FMP were inspected to determine if additional bathymetric data were required, and the Enfield model was the only FMP model for which additional field surveys were needed. Bathymetric data for the models developed entirely by the USGS were collected by USGS personnel from bridges and manned boats by using graduated survey rods in shallow streams and acoustic instruments in deeper creeks and rivers. A differential global positioning system (DGPS) was used to establish horizontal stationing.

The overbank topography for the FMP models, which was derived from a 6.1-m by 6.1-m DEM, was checked and compared to the 1.5-m by 1.5-m DEM developed by the USGS. Significant differences between the two DEMs were resolved by replacing the coarse-resolution DEM with the fine-resolution DEM. Overbank topography for the remaining models was developed from the 1.5-m by 1.5-m DEM.

Overbank cross sections for use in HEC–RAS generally are approximately perpendicular to the stream at the point the cross section intersects the stream, and each cross section intersects the main channel only once. In addition, two cross-section lines cannot intersect each other. Many of the streams in the study area are quite sinuous, so great care was required to develop overbank cross sections that met these requirements. Even so, there were cases, such as near the confluence of a tributary with the main channel, that it was not possible for the overbank cross section to be perpendicular to both the main channel and the tributary (for example, fig. 8). Although overbank cross-section locations were delineated manually for this study, the process has since been automated.

The geometry of structures, such as bridges and roadway elevations, in the FMP models was reviewed, potential problems were identified, and structural geometry was verified by land surveys as needed. Bridge and roadway geometries for the models created entirely by the USGS were determined by survey crews using an electronic total station supplemented with North Carolina Department of Transportation bridge plans, when available.

Combined, the Tar River hydraulic models included 272 km of streams in the basin, including about 162 km on the Tar River main stem (table 3). Cross-section density in the models was about one cross section per 400 m of stream length, with generally higher densities on tributary streams than on the main stem. The models also included the effects of 59 bridges on flow in the basin. Bridges can have a noticeable effect on water levels under certain conditions (for example, the water-surface profile at the Ward Road bridge across Little Fishing Creek in reference to a water-surface elevation of 43.43 m at the streamgage, fig. 9).

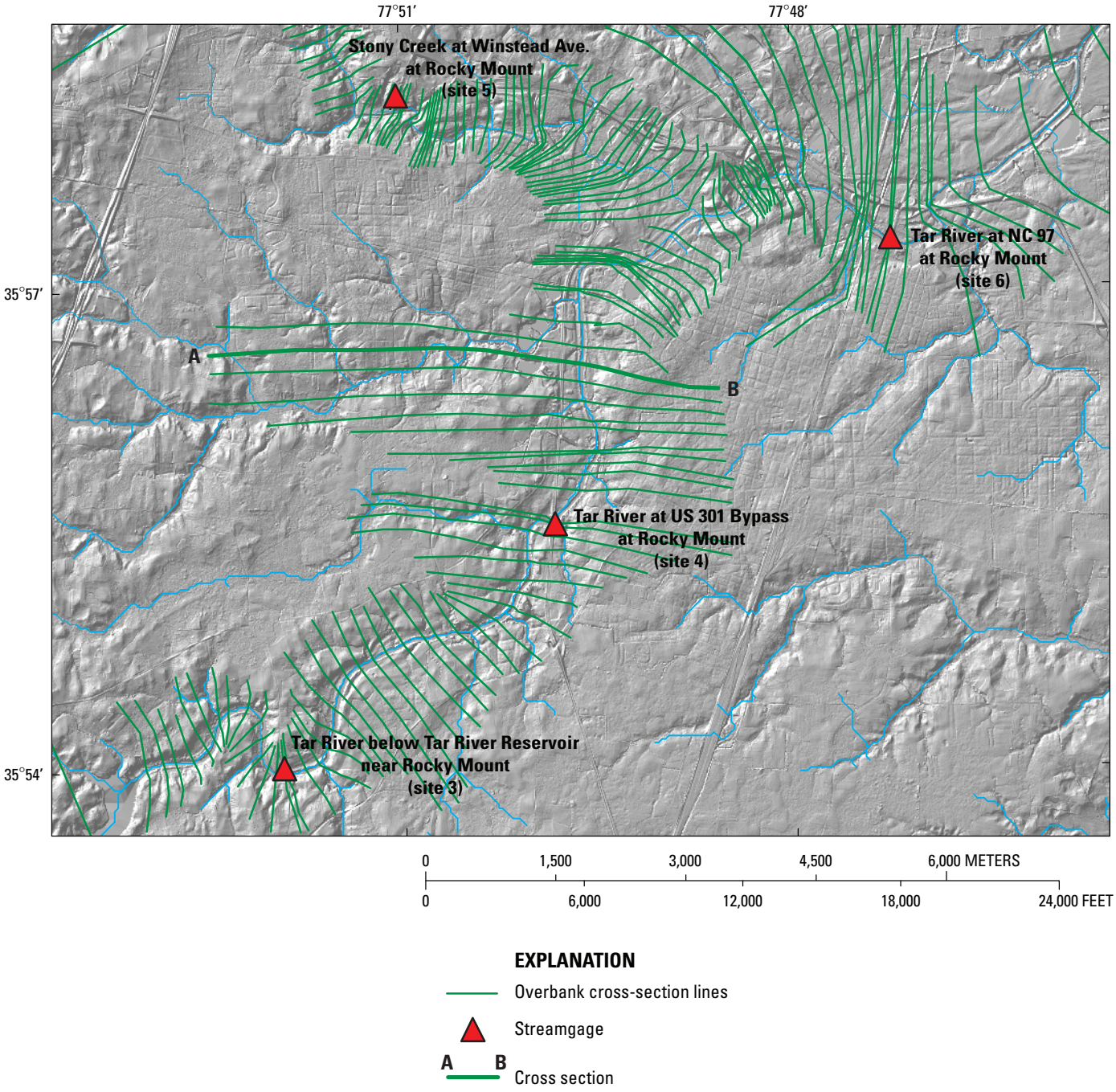

Figure 8. Overbank cross sections used in the Rocky Mount hydraulic model.

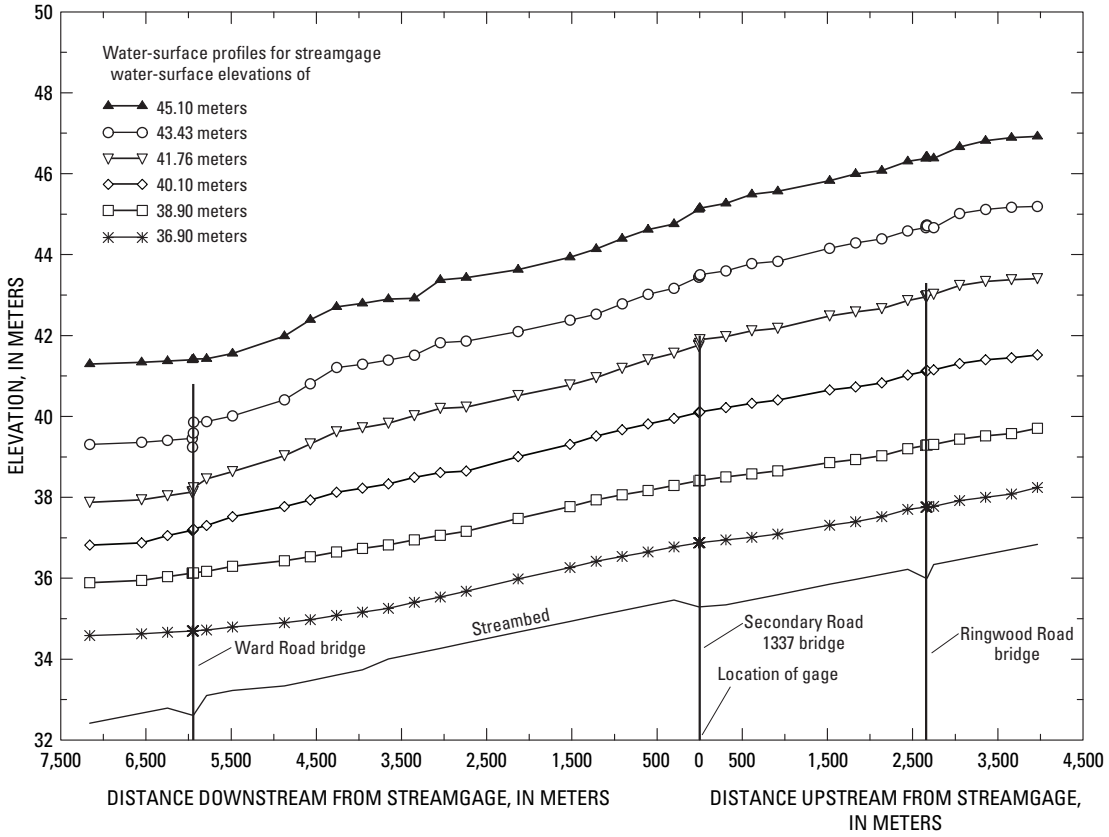

Figure 9. Simulated water-surface profiles for Little Fishing Creek near White Oak streamgage (site 9) in the Tar River basin, North Carolina.

Downstream Boundary Conditions—Nontidal Sites

Downstream boundary conditions for all models except the Grimesland and Washington models were established using the normal depth condition (Hydrologic Engineering Center, 2002, p. 7–4) with a friction slope estimated from the streambed slope through the reach. The normal depth is calculated by using the Manning equation with user-provided data for slope, geometry, and Manning's *n*. The Pinetops model boundary was extended downstream to include the Tar River, which affects flow at the Town Creek site under high-flow conditions.

Downstream Boundary Conditions—Tidal Sites

A normal-depth downstream boundary condition was not appropriate for the Grimesland and Washington models because the simulated flows can be affected by tides or backwater from the Pamlico River. Therefore, the approach for the Washington model was as follows. Stage and an index velocity were measured continuously at site 19 (fig. 1, Pamlico River at Washington), and a continuous record of discharge was computed. Records from this site were examined to identify dates of high ebb flow. The measured stage and computed discharge for these dates then were used to construct a stage-discharge rating for downstream (ebb) flows. This rating provides a reasonable estimate of the relation between stage and ebb flow at site 19 for the purposes of constructing a steady-flow model. A simple stage-discharge rating cannot be developed, however, over the full range of tidal conditions that occur at site 19.

The approach for developing the downstream boundary condition for the Grimesland model was different from the Washington model because discharge records were not available for site 17 (fig. 1, Tar River at SR 1565 near Grimesland). A stage-discharge rating for site 17 was established by successively interpolating known stages at sites 15 (Tar River at Greenville) and 19 (Pamlico River at Washington) to site 17, based on the water-surface slope between these two gages, for ebb-flow conditions at site 19. This estimated water-surface elevation at site 17 was then associated with the discharge at site 15 for a series of high ebb-flow conditions to establish a stage-discharge rating for the downstream boundary condition.

Upstream Boundary Conditions—Gaged Sites

Steady flow was the upstream boundary condition for all of the models. The full range of flows for the downstream rating curve was used as the upstream boundary condition for

all models that were calibrated by using downstream rating curves (table 3). Upstream flows for model calibration at other sites were based on either estimated flows at which high-water marks were established or flows at which discharge measurements were made. Upstream boundary conditions for development of water-surface profiles for inundation mapping were developed from the downstream rating curve or a synthetic rating curve as described below. Upstream flows were incrementally selected to provide a 0.305-m change in water level at the gage over a range of flows from approximately bankfull to the maximum recorded water level.

Upstream Boundary Conditions—Ungaged Sites

Synthetic stage-discharge relations were developed for sites 8, 11, 13, and 18 for which measured rating curves were not available (table 1). Synthetic rating curves were required to estimate the flows associated with the measured downstream discharge (sites 8 and 11) and high-water marks (sites 13 and 18) to which the models at these sites were calibrated. Flow and water level at these sites also can be affected by backwater from the Tar River, so this factor was considered in the development of the synthetic ratings. The approach for developing the synthetic rating curves was as follows, using site 8 (Swift Creek at NC 97 near Leggett) as an example.

A streamgage with long-term records in a basin with similar hydrologic characteristics as site 8 was identified. In this case, site 7 (fig. 1; table 1, Swift Creek at Hilliardston) was used. In addition, because site 8 can be affected by Tar River backwater, the nearest downstream Tar River streamgage was identified, which was site 12 (fig. 1; table 1, Tar River at Tarboro). A set of recent mid- to high-flow peak discharges (daily mean flow) was identified and compiled for site 7. The corresponding peak water-surface elevations at site 12 then were compiled, and a relation between peak flow at site 7 and peak water-surface elevation at site 12 was developed (fig. 10). The correlation coefficient for the relation between flow at site 7 and water-surface elevation at site 12 was 0.95, and the correlation coefficients for similar relations for the other three sites (11, 13, and 18) ranged from 0.82 to 0.99. The relation between flow at site 7 and water-surface elevation at site 12 was then used to estimate the flow at site 8 for a specified water-surface elevation in the Tar River at site 12. This was done by multiplying the discharge at site 7 by the ratio of the drainage area at site 8 to site 7.

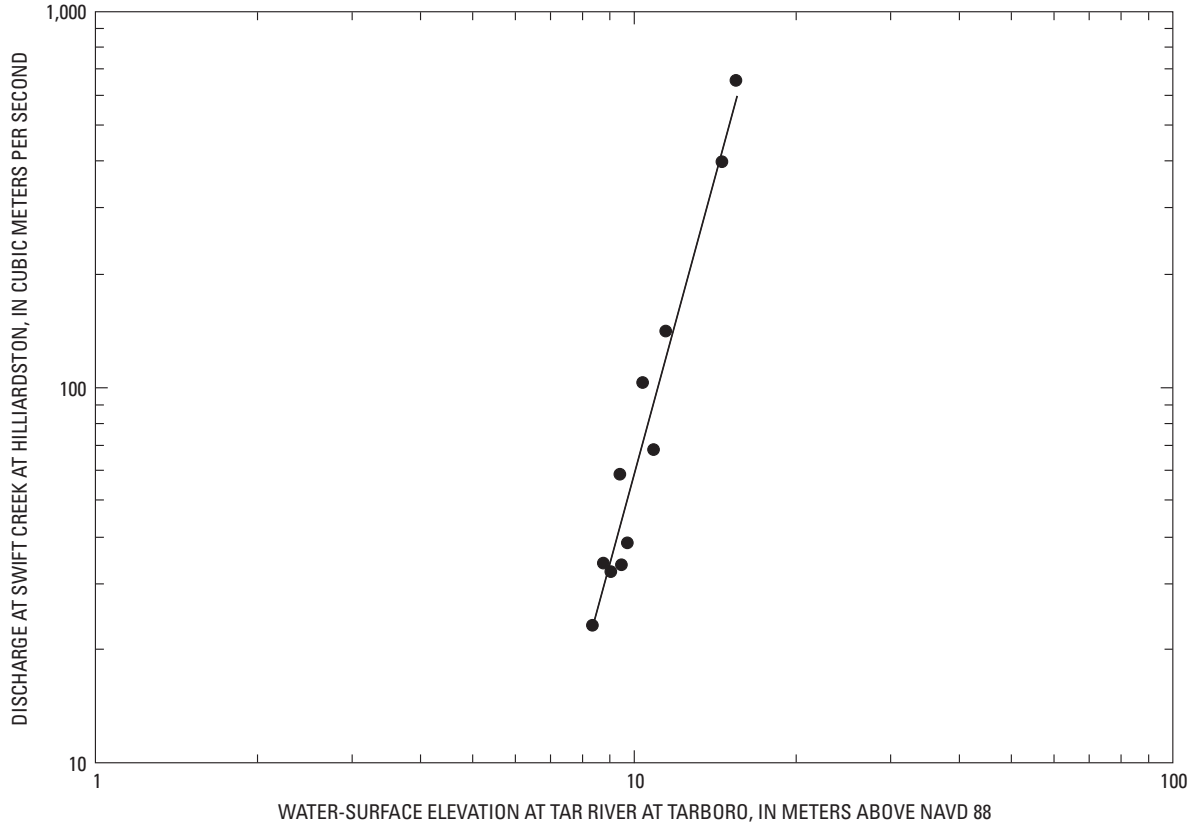

Figure 10. Relation of water-surface elevation at the Tar River at Tarboro (site 12) to peak flow at Swift Creek at Hilliardston (site 7), North Carolina.

Peak flows for a large regional flood occur earlier at site 8 than at site 12 because the drainage area at site 8 is substantially less than at site 12. Yet, the analysis described above assumes that the peaks on the tributary (site 8) and the Tar River (site 12) occur on the same day. A routing factor was therefore applied to the peak flow determined for site 8 to account for the fact that site 8 typically peaks before site 12. The routing factor was determined by computing the sum of the peak discharges for site 6 (the Tar River streamgage just upstream from site 12) and the gaged tributaries draining to the Tar River between sites 6 and 12. The ratio of this sum to the peak flow at site 12 was then the routing factor. Hence, for a given water-surface elevation at site 12, the flow at site 8 was (1) calculated from the relation of water-surface elevation at site 12 to flow at site 7 and adjusted for drainage area at site 8, as described above, and (2) multiplied by the routing factor to account for differences in peak arrival times at site 12. The discharge-water-surface elevation pairs determined in this manner then constituted the synthetic rating curve at site 8. A routing factor also was required for the Pinetops model (site 13).

The upstream boundary conditions for the Grimesland model were established in a slightly different manner. The two upstream boundaries for the Grimesland model are Chicod Creek and the Tar River. The drainage area at the Grimesland gage (site 17) is 6.9 percent greater than at the Greenville gage (site 15). Approximately 53 percent of the 6.9-percent drainage area increase is attributed to Chicod Creek, so inflow from Chicod Creek was equal to the measured flow at Greenville multiplied by 0.037 (53 percent of 6.9 percent). The flow in the Tar River at the upstream end of the Grimesland model was equal to the flow at Greenville multiplied by 1.032 (47 percent of 6.9 percent plus the flow at Greenville). The estimated water-surface elevation at site 17 (described above) was then associated with the computed discharge at site 17 for a series of high ebb-flow conditions to establish the synthetic stage-discharge rating for the upstream boundary condition.

Calibration and Performance

The hydraulic models were calibrated to the most current stage-discharge relations at 11 long-term streamgages where rating curves have been developed (table 3). Of the 19 gaging stations, however, 8 did not have established rating curves because the gages were installed as part of this project to collect only stage data. Medium- to high-flow discharge measurements were made at several of the eight sites (table 3), and high-water marks from Hurricanes Fran and Floyd were available for high-stage calibration (U.S. Army Corps of Engineers, 1997; Federal Emergency Management Agency, 2000). These data were not sufficient, however, to calibrate the models over the full range of flows at the eight sites for which no rating curves were available.

Sites 4 and 5 did not have measured rating curves, but these sites were within the Rocky Mount model (table 3), which included two other sites that did have measured rating curves. Calibration of the Rocky Mount model, then, primarily focused on matching measured and simulated stage-discharge ratings at sites 3 and 6. Limited discharge measurements and high-water marks subsequently were used to check model performance at site 4, which is physically between sites 3 and 6, and site 5. A similar approach was used for the Tarboro, Greenville, and Grimesland models. These models each contained one site with a measured stage-discharge relation (site 12 for the Tarboro model, site 15 for the Greenville model, and site 16 for the Grimesland model). These sites were the focus of the respective model calibrations. Performance of the Greenville and Grimesland models subsequently was tested at the two sites without stage-discharge relations (sites 14 and 17 for Greenville and Grimesland, respectively) using data from high-water marks.

Model calibration was accomplished by adjusting Manning's *n* values and, in some cases, channel cross sections and slope. Manning's *n* values varied among the cross sections; the highest values were in the floodplains (table 3). Extremely high Manning's *n* values were required on the outer edges of the floodplains in order to achieve calibration over the full range of flows for some of the models provided by the FMP. It is likely that these high values were needed because the spacing between channel cross sections in the FMP models was much greater than in the USGS models and because the FMP models were constructed for the highest flows, whereas the USGS models were constructed for a greater range of flows.

Models were calibrated for water levels ranging from approximately bankfull at the streamgage to flow at the 500-year exceedance level or to Hurricane Floyd peak stages, whichever was greater. The mean difference between the lowest and highest simulated water level was 5.7 m for the 11 models (table 3). The correlation coefficients between measured and simulated rating curves at 9 of the 11 sites with measured rating curves were 0.99 (table 4), and simulated rating curves matched measured curves over the full range of flows (fig. 11). Differences between measured and simulated water levels for a specified flow were no more than 0.44 m and typically were less. Differences between measured and simulated water levels for models calibrated to high-water marks were less than 0.25 m. These results demonstrate that the 11 Tar River models are capable of simulating accurate water levels over a wide range of flows in the Tar River and tributary streams.

Table 4. Summary of hydraulic model performance for sites in the Tar River basin of North Carolina.

[m, meter; —, no data]

Model	Site no. (fig. 1)	Calibration results					
		High-water marks		Field measurements		Measured stage-discharge rating curve	
		Number	Error[a] (m)	Number	Error[a] (m)	Correlation coefficient	Range in error[b] (m)
Tar River	1	—	—	—	—	0.9997	-0.41 – 0.06
Louisburg	2	—	—	—	—	0.9924	-0.44 – 0.38
Rocky Mount	3	—	—	—	—	0.9999	-0.34 – 0.36
	4	—	—	—	—	—	—
	5	2	-0.20, 0.14	1	0.15 m	—	—
	6	—	—	—	—	0.9990	-0.19 – 0.23
Hilliardston	7	—	—	—	—	0.9770	-0.37 – 0.51
Little Fishing	9	—	—	—	—	0.9936	-0.30 – 0.31
Enfield	10	—	—	—	—	0.9618	-0.35 – 0.37
Tarboro	8	—	—	—	—	—	—
	11	—	—	—	—	—	—
	12	—	—	—	—	0.9994	-0.04 – 0.30
Pinetops	13	1	-0.12	1	0.3 m	—	—
Greenville	14	—	—	—	—	—	—
	15	—	—	—	—	0.9981	-0.28 – 0.18
Grimesland	16	—	—	—	—	0.9962	-0.13 – 0.13
	17	1	0.12	5	-0.13 – 0.27 m	—	—
Washington	18	1	0.23	—	—	—	—
	19	—	—	—	—	0.9954	-0.20 – 0.23

[a]Measured water level minus simulated water level.

[b]For a given discharge, water level from rating curve minus simulated water level.

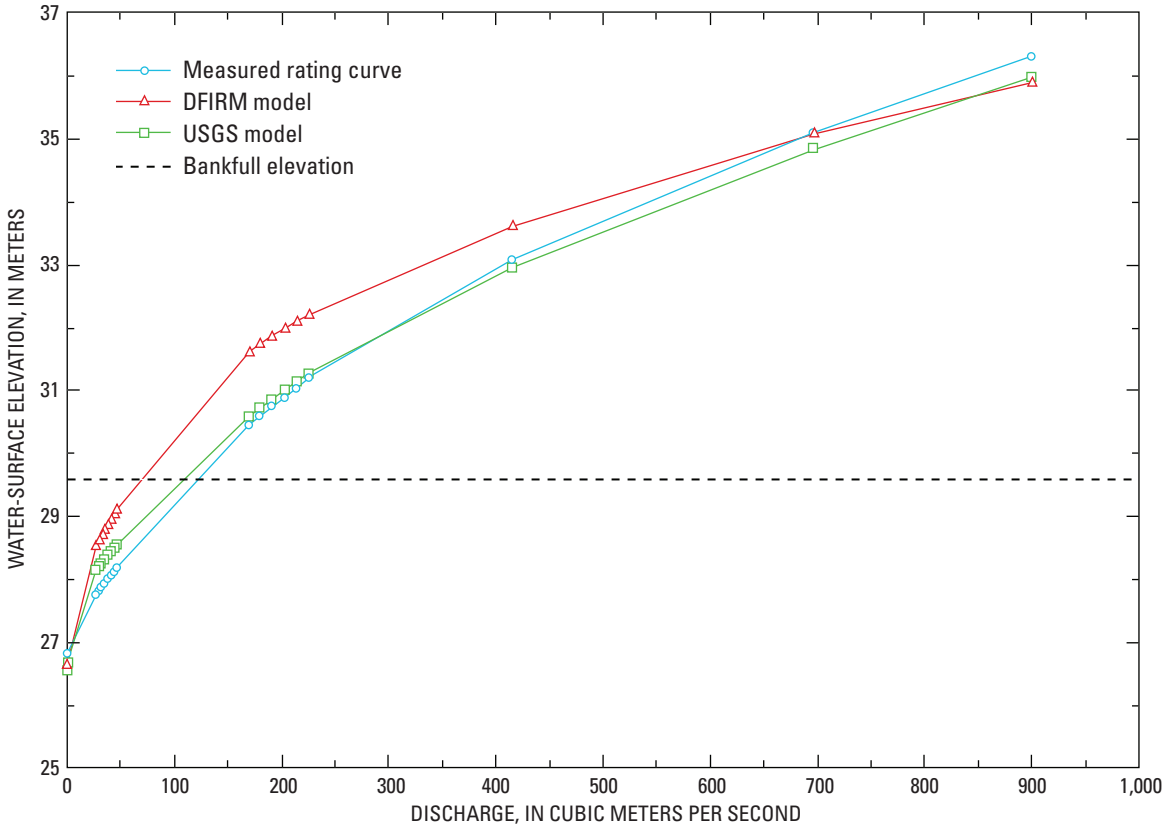

Figure 11. Measured and simulated stage-discharge relations for Swift Creek at Hilliardston (site 7) in the Tar River basin, North Carolina.

Flood-Inundation Maps

A set of water-surface profiles was generated for each of the 11 modeled reaches. The water-surface profiles were generated at 0.305-m increments for water levels ranging from bankfull to approximately the highest recorded water level at the downstream-most gage in each modeled reach. For a given water-surface elevation at the downstream-most gage in the modeled reach, a water-surface elevation was assigned to each cross section in the reach (for example, fig. 8) at the point the cross section intersected the main stem of the modeled reach. The water surface was assumed to be level across the entire cross section, which is consistent with the one-dimensional modeling approach. Water-surface elevations between cross sections were estimated by using a spline interpolation (fig. 12).

Inundated areas were identified by subtracting the water-surface elevation in each 1.5-m by 1.5-m grid cell from the land-surface elevation in the cell (fig. 12). Because all inundated cells were not necessarily hydraulically connected to the flooded river or stream, an automated procedure was developed to identify all inundated cells that were hydraulically connected to the cell at the downstream-most gage in the model domain. All other inundated cells were deleted from the map layer. This entire process was repeated for each of the 0.305-m increment water-surface profiles in each model domain, creating 11 sets of inundation-map libraries (table 5). The number of inundation maps per modeled reach ranged from 10 to 28 and was a function of the range in water levels at the site. An example of metadata for the inundation maps is given in the appendix of this report.

The inundation polygons can be merged with a variety of other geospatial data to provide useful information for addressing flood mitigation or planning emergency response. For example, the inundation polygon can be combined with a topographic relief image to show the river channel through the inundated area and to depict inundation in relation to various topographic features in the area (fig. 13). Care must be taken in interpreting this type of image, however. In some cases, bridges appear to be inundated; for example, note the red circle in figure 13. In fact, this particular case is an example of hydroconditioning of the DEM, as discussed previously, in that the bridge is artificially cut so that the segments of the river upstream and downstream from the bridge are hydraulically connected. The yellow circle in figure 13 shows an area in which the road is actually inundated. This problem can be resolved by using the hydroconditioned DEM for mapping the inundation and then reintroducing the preconditioned DEM for depiction of potential transportation disruptions.

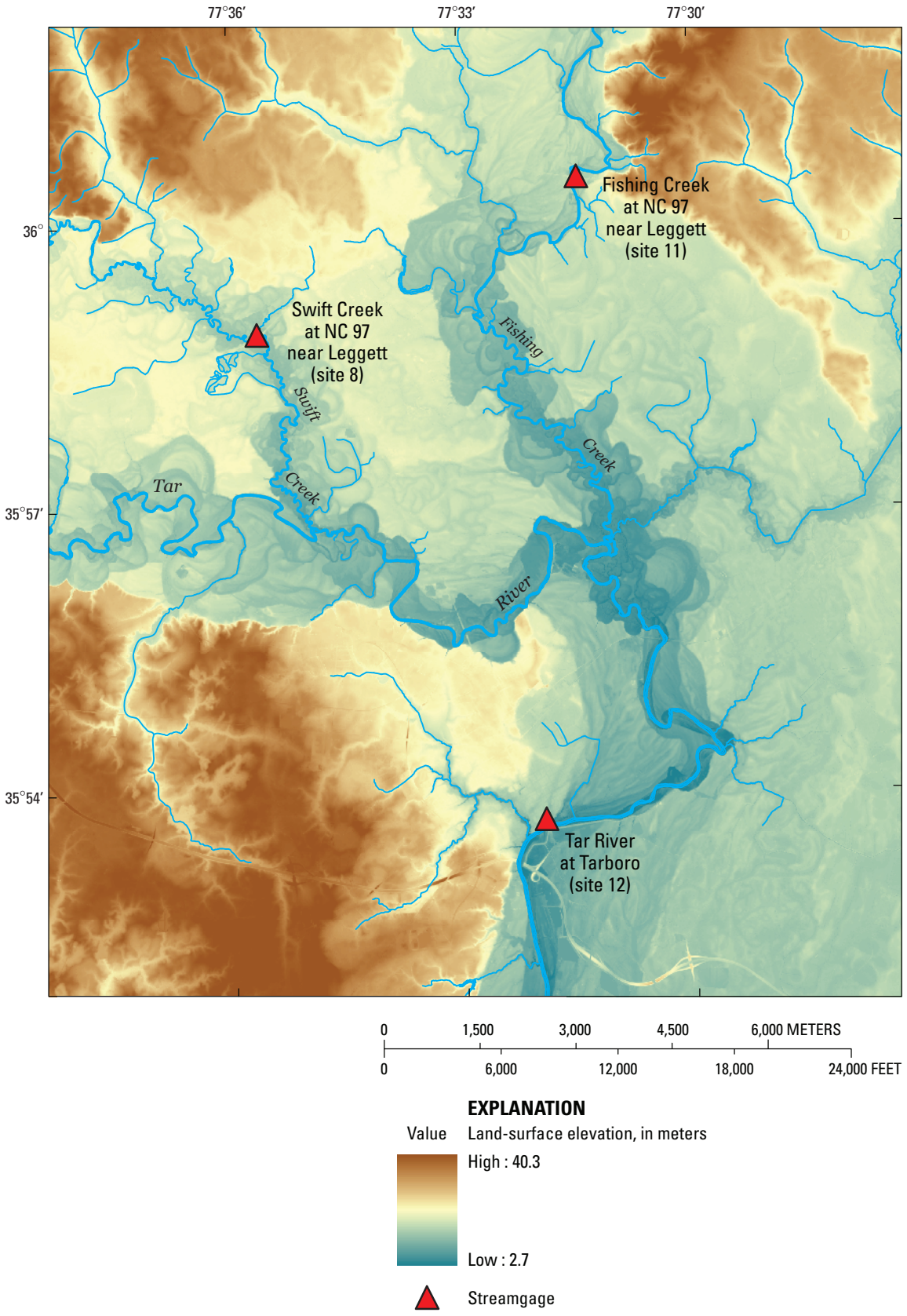

Figure 12A. Land-surface elevation for the Tarboro model.

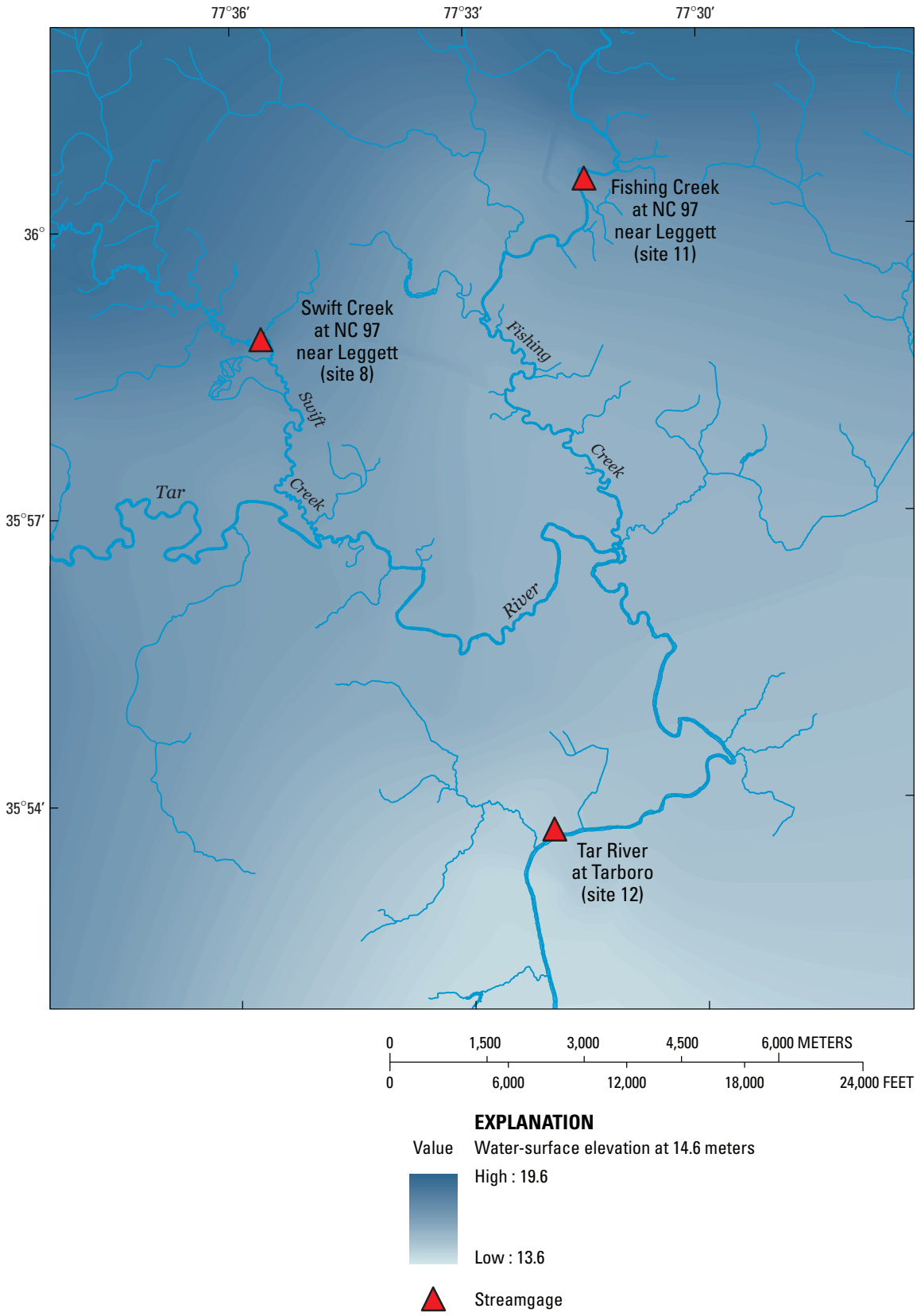

Figure 12B. Estimated water-surface elevation for the Tarboro model.

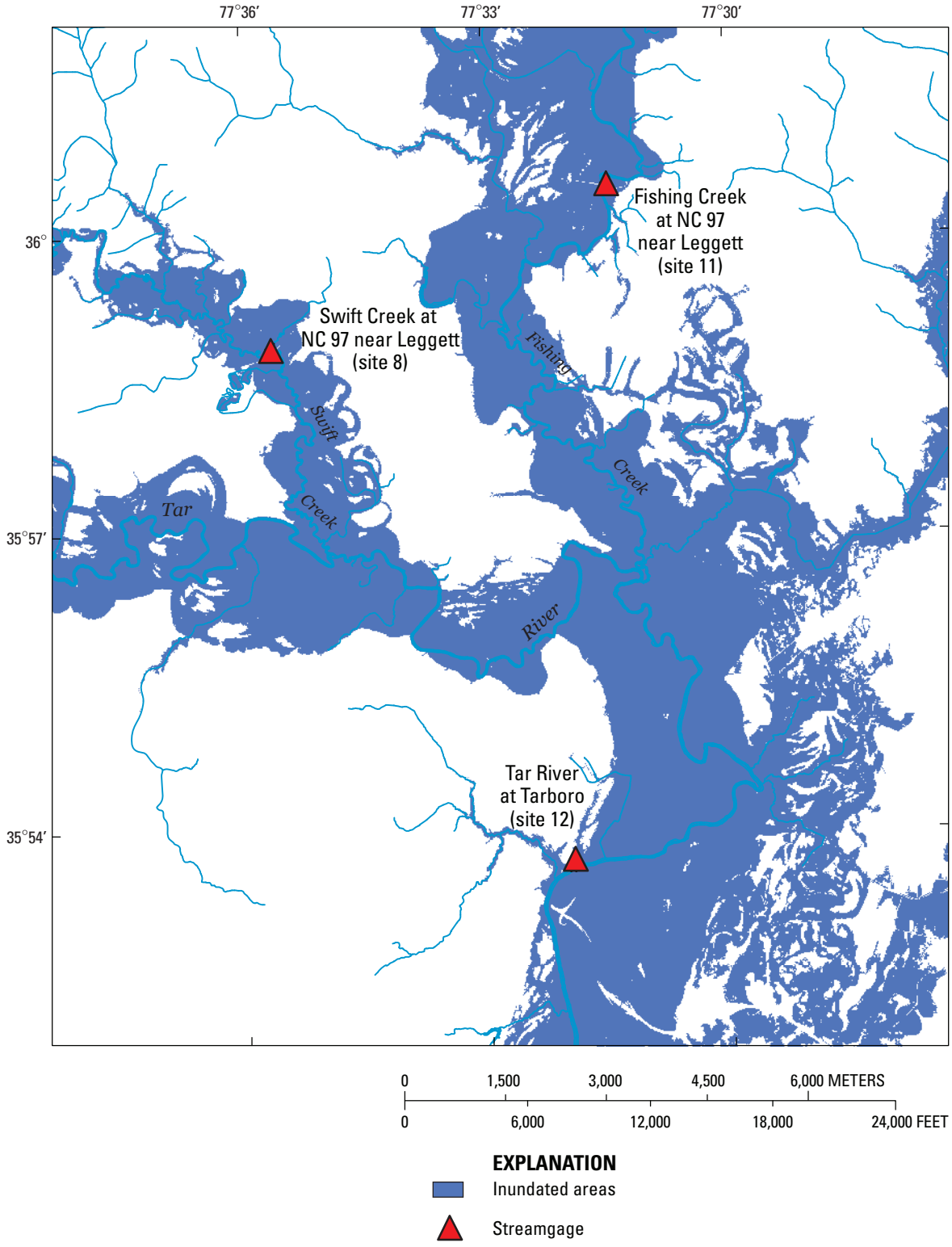

Figure 12C. Inundated area for the Tarboro model.

Table 5. Inundation-map libraries for the Tar River basin in North Carolina.

[m, meter; NAVD 88, North American Vertical Datum of 1988]

Model	Sites (fig. 1)	Number of maps for model domain	Range in water-surface elevation for map library		Site to which water levels are referenced
			Minimum (m above NAVD 88)	Maximum (m above NAVD 88)	
Tar River	1	25	88.1	95.4	1
Louisburg	2	23	55.8	62.5	2
Rocky Mount	3, 4, 5, and 6	23	29.6	36.3	3
Hilliardston	7	18	41.1	46.3	7
Little Fishing	9	28	36.9	45.1	9
Enfield	10	15	24.8	29.1	10
Tarboro	8, 11, and 12	26	8.4	16.0	12
Pinetops	13	25	9.8	17.1	13
Greenville	14 and 15	21	1.8	7.9	15
Grimesland	16 and 17	21	-0.3	5.8	17
Washington	18 and 19	10	-0.2	2.6	18

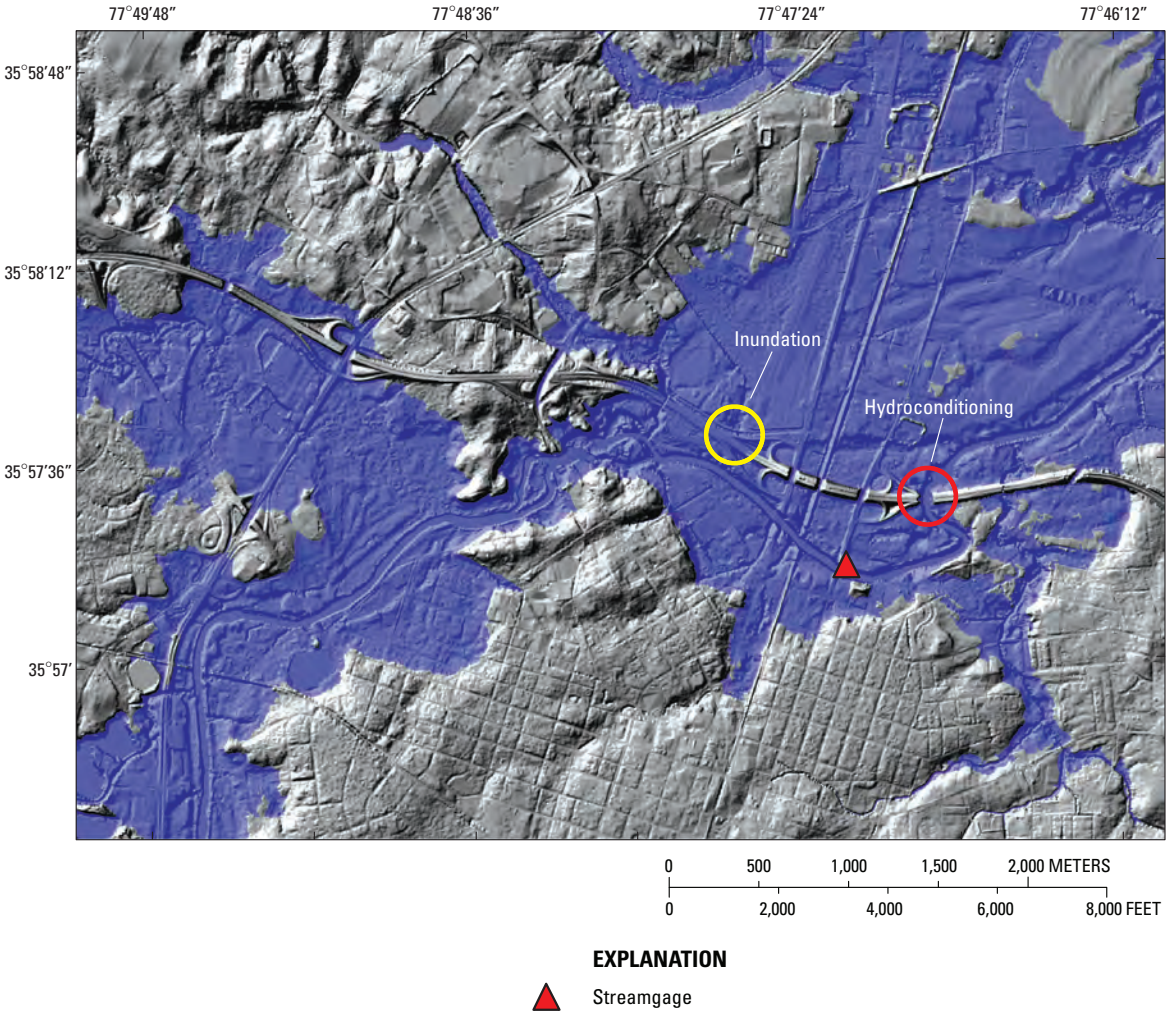

Figure 13. Inundation map showing topographic relief for the Tar River at NC 97 at Rocky Mount (site 6) for a water-surface elevation at this site of 38.6 meters above North American Vertical Datum of 1988.

Transportation networks can be superimposed on the shaded relief map and inundation polygon to better identify roads affected by floodwaters (fig. 14). The use of orthoimagery with the inundation maps provides further information on flooded or potentially flooded structures, agricultural lands, and other areas of interest (fig. 15). Finally, the water-surface elevations throughout the inundated area can be combined with land-surface elevation data to depict estimated water depth (fig. 16).

Low-resolution inundation maps showing transportation networks and orthoimagery have been prepared for display on the Internet (U.S. Geological Survey, 2006c). These maps also are linked to USGS real-time streamflow in the National Water Information System database (for example, U.S. Geological Survey, 2006b). Hence, a user can determine the near real-time stage and water-surface elevation at a USGS streamgage site in the Tar River basin and link directly to the flood-inundation maps to obtain a depiction of the estimated inundated area at the current water level.

Uncertainty Associated with Inundation Maps

Although the flood-inundation maps represent the boundaries of inundated areas with a distinct line, some uncertainty is associated with these maps. Because of this uncertainty, flood boundaries more reasonably could be replaced with zones depicting probability of flooding (Brown and Damery, 2002). Moreover, uncertainty varies, depending on the scale at which the inundation modeling is conducted (Horritt and Bates, 2001). There are a number of methods for estimating uncertainties associated with hydraulic modeling and inundation mapping, but data required to apply these methods are seldom available (Beven, 2006), which is true in this case. Nevertheless, uncertainties in the Tar River basin inundation maps can be discussed in a qualitative manner, which is the purpose of this section.

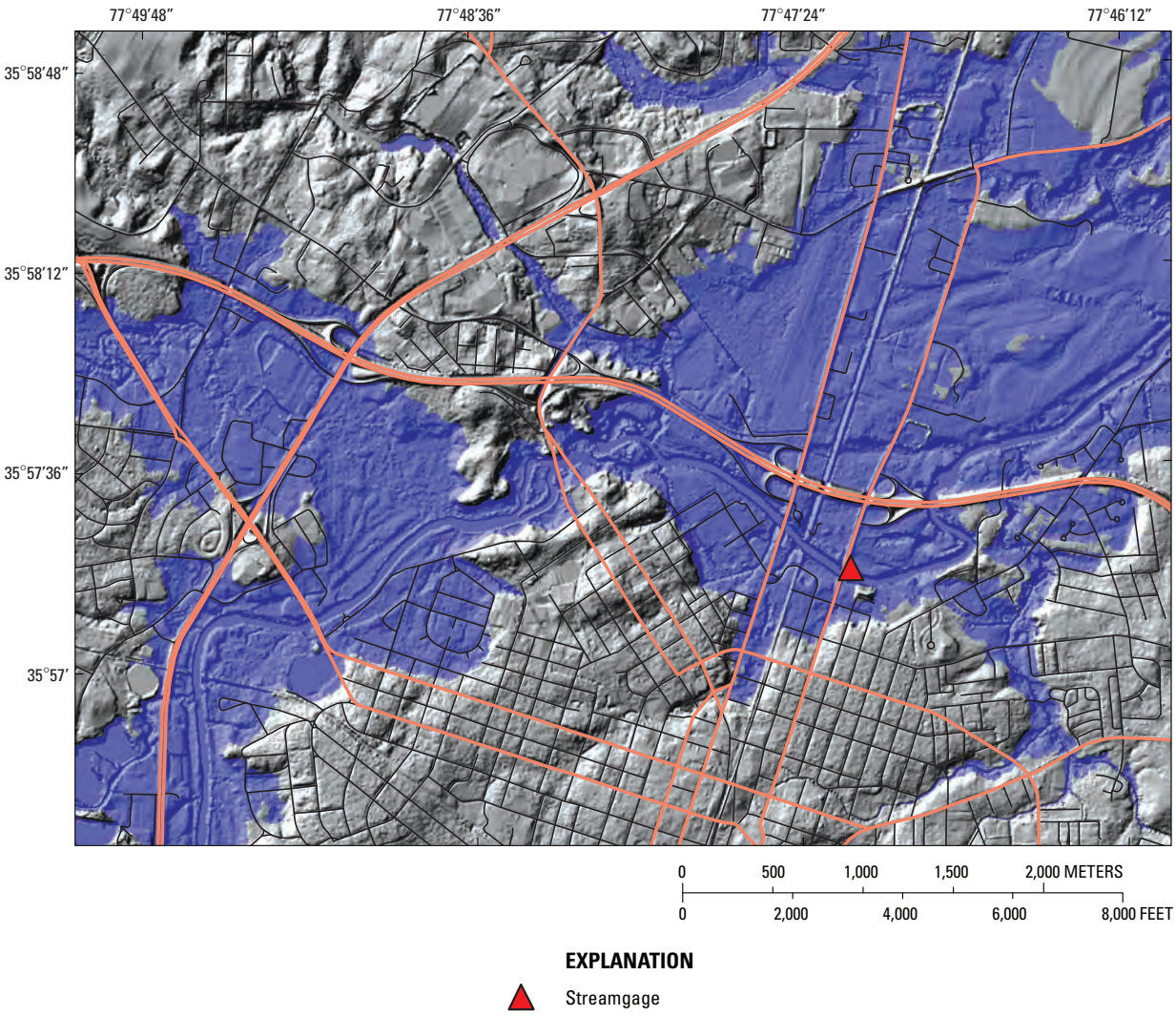

Figure 14. Inundation map showing topographic relief and transportation networks for the Tar River at NC 97 at Rocky Mount (site 6) for a water-surface elevation at this site of 38.6 meters above North American Vertical Datum of 1988. (Transportation networks from North Carolina Department of Transportation, 2006)

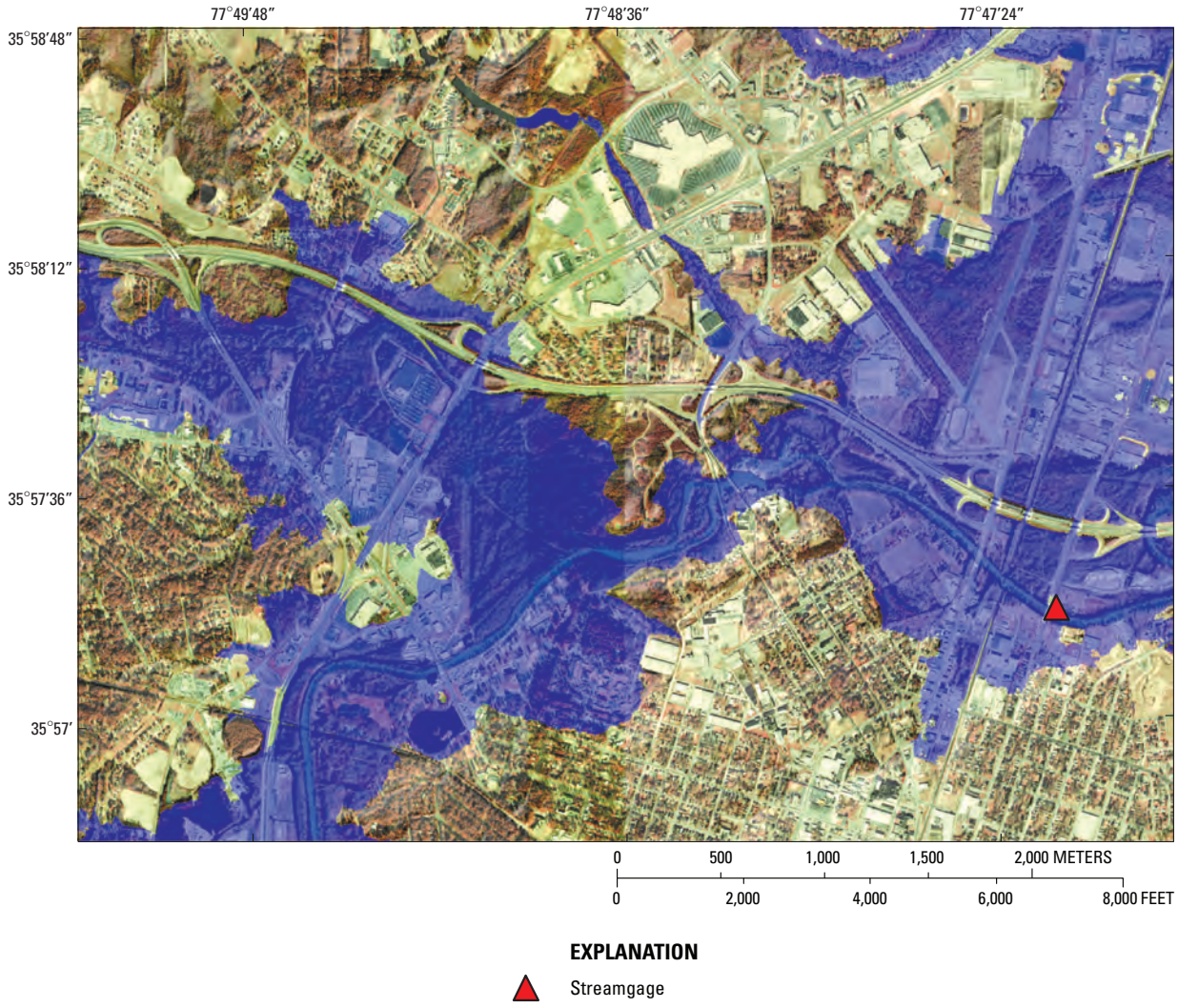

Figure 15. Inundation map showing orthoimagery for the Tar River at NC 97 at Rocky Mount (site 6) for a water-surface elevation at this site of 38.6 meters above North American Vertical Datum of 1988. (Orthoimagery from the U.S. Geological Survey, 2006a)

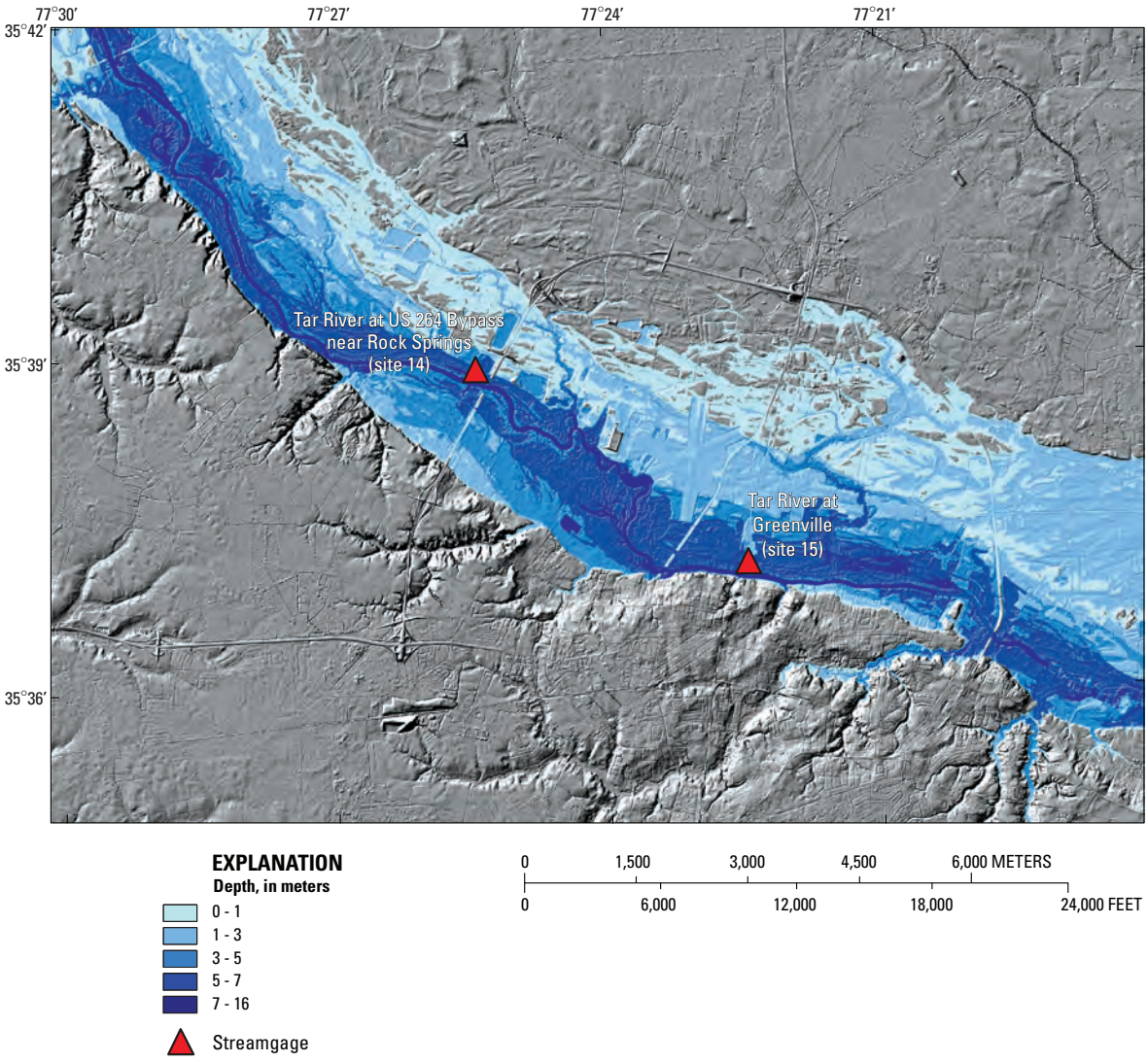

Figure 16. Estimated floodwater depth for the water-surface elevation of 7.9 meters above North American Vertical Datum of 1988 in the Tar River basin at Greenville, North Carolina.

Data for Model Development and Calibration

Flood-inundation models require three types of data—(1) topographic data for the hydraulic model computational grid and the inundation maps; (2) effective friction values (Manning's *n*) for each computational segment (one-dimensional model) or cell (two-dimensional model); and (3) model-validation data of some type (Bates, 2004), and each of these data types has uncertainties. Models applied in near real time also require a forecast hydrograph.

As previously noted, the root mean square error in the Tar River basin land-surface elevation data was about 0.2 m. Land-surface elevations, or topography, is the dominant influence on the location of the simulated shoreline of an inundated area. Other studies have demonstrated that low-resolution one-dimensional hydraulic modeling combined with high-resolution topographic data gives a good representation of shoreline (Horritt and Bates, 2001), which is the reason the original LiDAR data were reprocessed to provide 1.5-m horizontal resolution topographic data.

Inundation maps for selected flows produced by using the 1.5-m grid cells for the Tar River at Tarboro were compared with maps produced by using the 6.1-m horizontal resolution cells. Inundated areas for streamflow at the 100-year exceedance level differed markedly for the two DEMs; the fine-resolution topography showed a much larger inundated area than the coarser resolution topography. Further analysis indicated that the 6.1-m grid cell topography depicted a roadway as a barrier to flow, whereas the 1.5-m grid cell topography depicted flow over the roadway. Ground surveys subsequently confirmed that the 1.5-m cell topography properly represented the roadway.

Friction values, or Manning's *n*, are effective in that they account for the effects of variable cross sections, nonuniform

slope, vegetation, and structures at the scale of the distance between model cross sections. Distributed data throughout the floodplain are seldom available as a basis for estimating friction values for the entire model domain. Studies also have shown that many different model-parameter sets can perform equally well in HEC–RAS (Pappenberger and others, 2005a), which represents uncertainty in the model, regardless of the goodness of fit between measured data and simulated values. Moreover, the Manning formula was developed for uniform flow, which is not present during floodflows, and the equation is dimensionally nonhomogeneous. Hence, many of the uncertainties in one-dimensional hydraulic models are included in the Manning *n* value. Extreme care must be used when developing these models to ensure that the Manning *n* value is not used to compensate for errors in other aspects of the model in order to achieve model calibration.

The HEC–RAS model can be calibrated adequately at a single point by using a time series of stage and discharge (Horritt and Bates, 2002). The models, however, are used to simulate an inundated area, so calibration at a single point is not really an adequate calibration. Moreover, the extent of an inundated area alone may not be sufficient to evaluate model performance, particularly for flat floodplains (Hesselink and others, 2003).

Adequate calibration data are seldom available for inundation models. Although the models are used to provide estimates of the shoreline throughout the inundated area, the models typically are calibrated measurements and simulations at a single, or perhaps a few locations. In addition, streamgage data can be in error by as much as 20 percent or more during extreme floods, so improved methods for monitoring floodflows are needed (Bates and others, 2006). An ideal data set for flood-inundation model calibration and validation would include spatially detailed data for the inundation shoreline and, if the models are used to provide estimates of inundation depth, data for water depth throughout the model domain.

Several approaches have been attempted to obtain inundation model-validation data sets. Puech and Raclot (2002) developed a unique approach to estimate inundation water depth from aerial photographs, but the approach likely is not applicable to North Carolina floodplains because the floodplain must be broad and divided by numerous natural elements, such as dikes and levees. Other remote-sensing approaches include the following:

- SPOT satellite and RADARSAT images were used to classify inundation areas data (Toyra and others, 2002). Accuracies increased from 70 to 80 percent, and one method alone increased accuracy to greater than 90 percent with combined use of the two images. Pixel size was 10–20 m.

- Successive LANDSAT Thematic mapper images with resolutions of 30 m by 30 m were used to develop a model of flood growth in a 600-km-long river, but problems with water turbidity, dense riparian vegetation, and cloud cover were common (Overton, 2005). LANDSAT images also were used to develop an inundation map of the Tar River in Pitt County following Hurricane Floyd (Wang and others, 2002), but images were not available until 9 days after the flood crested.

- Advanced very high resolution radiometer (AVHRR) data were used to delineate flood inundation during the major floods of 1988, 1995, and 1999 in Bangladesh. AVHRR resolution, however, is 1.1 km and is available only during cloud-free periods, and ground control points are needed to correct for geometric distortion (Islam and Sado, 2002).

- RADARSAT synthetic aperture radar (SAR) was used to map inundation in the Roanoke River floodplain of North Carolina. Mapping was approximately 94 percent accurate and was 90 percent accurate when the water level was between minus 10 cm and plus 10 cm of the ground surface (Townsend, 2001). SAR can be used regardless of cloud cover or vegetation conditions, but data are available only at 7- to 10-day intervals. Bates and others (2006) collected four SAR images from an aircraft during a flood event on River Severn in England. Resolution of the images was 1.2 m, and streamgage data also were available. This is, perhaps, the most extensive flood-verification data set available.

Steady-Flow Versus Unsteady-Flow Modeling

The Tar River flood-inundation maps were developed by using a steady-flow hydraulic model. This means, for example, that if an inundation map were developed for the Tar River at Tarboro (site 12, fig. 1) for a flow of 1,000 m^3/s, it could be assumed that the flow at Tarboro would be a constant 1,000 m^3/s for a sufficient period to allow all land areas that could be flooded at that flow to become inundated. This assumption clearly has less of an effect on inundation maps produced for lower flows than for higher flows, because more time typically is required to inundate areas at high flows than at low flows. Moreover, two floods at a given location having the same peak flow can have distinctly different inundation patterns. A flood in which water levels rise slowly to the peak and then fall slowly likely will result in more inundation than a flood with the same peak flow but in which water levels rise and fall quickly.

The Tarboro model (table 3) was used to investigate the effects of unsteady-flow simulations (Hydrologic Engineering Center, 1993) on estimates of flood inundation by simulating the Hurricane Floyd flood flows during September 1999 (fig. 17). The relation between the measured water level and simulated discharge at the site during the flood is shown in figure 17A. The arrows on the curve indicate rising or falling stage. For example, four different water levels were associated with a flow of 360 m^3/s (fig. 17A) occurring on September 9 during a rising water level, September 14 during falling stage,

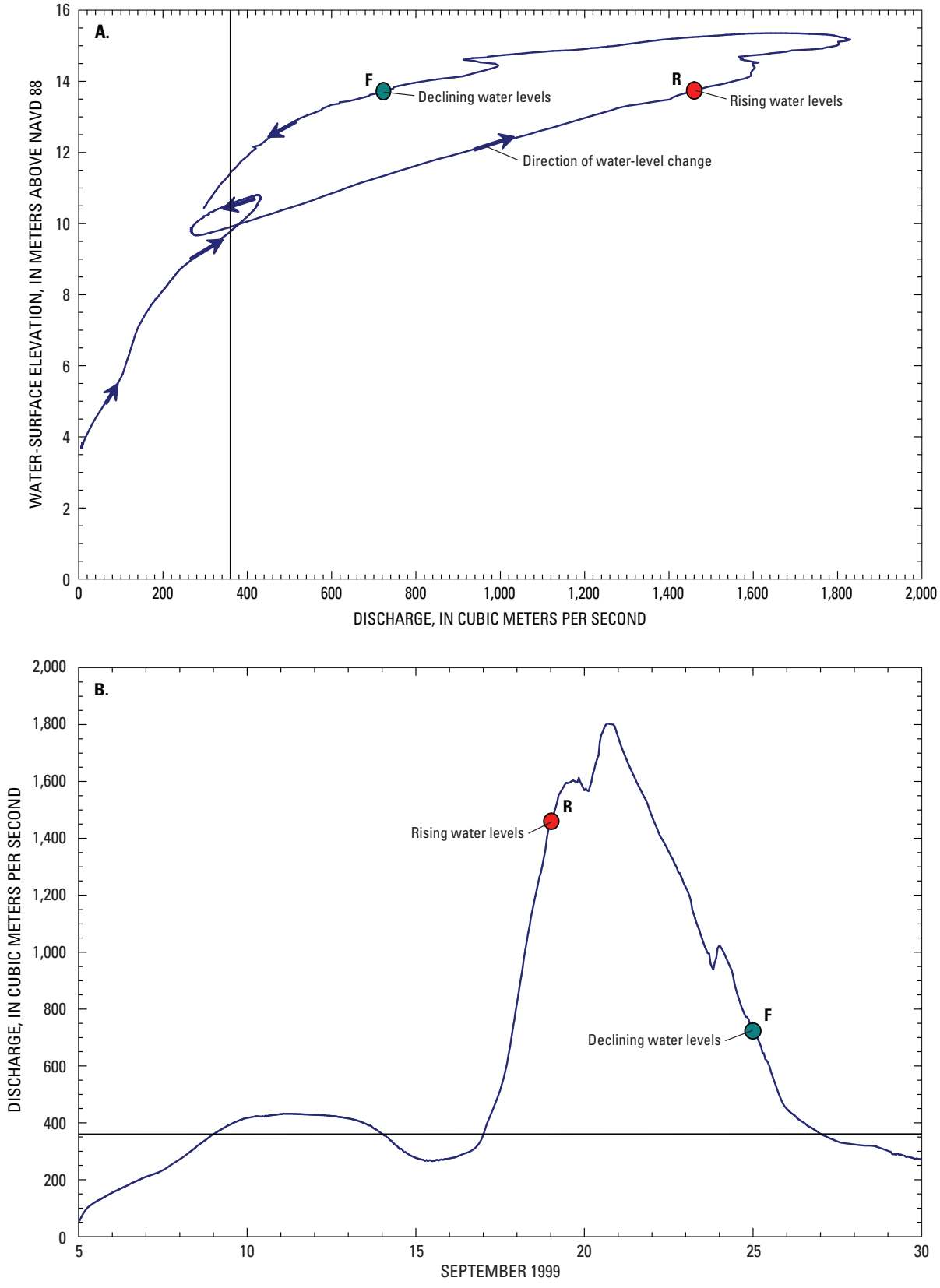

Figure 17. (A) Relation of measured water level and simulated discharge and (B) simulated hydrograph for the Tar River at Tarboro, North Carolina, during Hurricane Floyd flood, September 5–30, 1999.

September 17 during rising stage, and on September 27 during falling stage (fig. 17B). Water-surface elevations on these dates were 9.71, 10.55, 9.90, and 11.45 m above NAVD 88, respectively, a range of about 1.7 m. Hence, an inundation map for a flow of 360 m^3/s could have been selected from among seven different maps (9.7, 10.0, 10.3, and so on to 11.3 m above NAVD 88).

The peak flow for a given exceedance level seldom occurs during steady-flow conditions, yet DFIRMs and inundation maps typically are created by assuming steady-flow conditions. Failure to attain steady-flow results in variable inundation extents for a single river flow (or stage), because a stable distribution of water in the floodplain is not attained. Additional research is needed on the relation between attainment of steady flow and the lateral distribution of water in the floodplain. Hence, the use of inundation maps to estimate inundation that may occur during, for example, a 50-year flood must be done with recognition of the uncertainties in the maps.

The Hurricane Floyd simulated hydrograph also demonstrates that flows of distinctly different magnitudes can occur for a given water level (fig. 17B). As water levels rose, a flow of 1,460 m^3/s occurred at a water-surface elevation of 13.7 m (R in fig. 17) on September 19, whereas the flow at the same water-surface elevation during falling water levels was 723 m^3/s on September 25 (F in fig. 17), or less than half the flow at the same water level. The Tarboro hydraulic model was applied to the unsteady flows during September 5–30, 1999, to estimate inundated areas. According to the simulations, the inundated areas for the two water-surface elevations of 13.7 m differed by more than 70,000 square meters (m^2), with more area inundated on September 25 (falling water level), despite the fact that the flow was less than half the flow at the same water level on the rising side of the hydrograph. These limitations associated with the steady-flow assumption for hydraulic modeling vary from site to site.

The alternative to using the steady-flow assumption and developing inundation-map libraries, as was done for this project, is to estimate inundated areas in real time during or immediately prior to a flood so that particular characteristics of the rainfall and flood hydrograph are well represented in hydraulic modeling. Research applications have demonstrated that it is possible to produce reasonable inundation maps from medium range weather forecasts (Pappenberger and others, 2005b) or from NWS estimates of rainfall derived from NEXRAD weather radar (Whiteaker and others, 2006). The limitation of this approach is that the models must be operating in real time for each event and that results must be distributed quickly to emergency management officials and all other interested parties. Moreover, there is some uncertainty in the forecast flows in the reach for which the inundation modeling is being conducted (Bates, 2004). The infrastructure and funding for such a system is not in place for the Tar River basin, nor is it available for most locations in the United States. (Fort Collins, Colorado, is a notable exception; Fort Collins Office of Emergency Management, 2006.) Hence, the steady-flow assumption, map-library approach was used in this study. Further studies are needed to document any benefits of the real-time system over the map-library approach and to demonstrate the conditions for which each approach is most applicable.

One-Dimensional Versus Two-Dimensional Modeling

The one-dimensional modeling approach used in this study resulted in good agreement between measured and simulated stage-discharge ratings at sites where these ratings were available, and good agreement between measured and simulated stage and discharge observations at other sites. One-dimensional models are relatively easy to construct, and simulations can be made quickly. One-dimensional hydraulic models are based on the assumption that the hydraulic variables (water-surface elevation, water-surface slope, velocity, and cross-sectional flow area) are uniform across a transect and that primary variations in these variables are from upstream to downstream. This assumption is reasonable for a prismatic channel in a relatively narrow floodplain.

The limitations of the one-dimensional approach can be seen, however, in section A–B in figure 8. Water levels are assumed to be constant across cross section A–B, but the cross section intersects streams other than the Tar River at five locations, where according to the one-dimensional assumption, water levels are the same as in the Tar River. It is possible to build branching one-dimensional models, as was done in the Rocky Mount model, which included Stony Creek and the Tar River, to partially avoid the problems associated with the one-dimensional assumption. It is not possible, however, to avoid the problems altogether, as even Stony Creek cross sections intersect multiple streams in some locations (fig. 8). The conclusion from this discussion, then, is that uncertainty in the flood-inundation polygons increases with distance from the main channel for which water-surface slopes were simulated, particularly in broad floodplains with numerous tributaries.

Two-dimensional models are being used increasingly for simulation of floodplain inundation because of variability in topography across the floodplain, particularly in wide floodplains with numerous tributaries. The results of previous studies have demonstrated that correct simulation of water storage in a floodplain near a channel is important for predicting flood-wave timing, and the increased lateral resolution of a two-dimensional model allows proper simulation of this process (Horritt and Bates, 2001). Raster models, which use a one-dimensional representation of channel flow linked to a simple model of flow between grids of cells on the floodplain, have been used to improve spatial resolution of flood inundation without significantly increasing computational requirements of the hydraulic model (for example Bates and De Roo (2000)). A coupled one-dimensional and two-dimensional model was used to develop a library of flood-inundation polygons for the Blue River, Missouri, where backwater from

the Missouri River affects flows in the Blue River (Kelly and Rydlund, 2006). Two-dimensional models are particularly appropriate for simulating a flood hydrograph. Jones and others (2002) used a fine-scale two-dimensional model to simulate the movement of a NWS forecast flood hydrograph through the Snoqualmie River valley in Washington to produce forecast inundation along a 28-km reach of the river.

The raw LiDAR data that were processed to provide topographic information for the Tar River inundation modeling also can be processed to provide other information that could be useful for two-dimensional modeling. For example, Cobby and others (2001) used LiDAR data to not only delineate the floodplain topography for a two-dimensional model but also to estimate vegetation height, which typically would be used in a flood-inundation model to determine friction coefficients. Different algorithms are used for different types of vegetation.

Summary and Conclusions

Flooding from Hurricane Floyd and other recent hurricanes in North Carolina clearly demonstrated that there is a growing need for more and better flood information, including products that (1) are available for more locations, (2) provide mapped information showing actual or predicted inundated areas, and (3) interface with a full suite of other flood-related products, such as DFIRMs and flood-forecast products produced by the NWS. In 2000, the FMP began a multiagency program to improve the flood information and flood-forecasting system for the State, with a long-term goal of providing emergency managers and the public more accessible, informative, timely, and accurate flood information and flood-forecast products for more locations. One of the primary roles of the USGS in this effort is to develop and demonstrate the technology for producing detailed flood-inundation maps for the Tar River basin. The maps can be used in conjunction with real-time streamgage measurements to depict current flooding and to provide estimates based on NWS flood forecasts of areas that are expected to become inundated.

Data from 19 streamgages in the Tar River basin upstream from (and including) Washington were used in this study. Five of the sites are NWS flood-forecast points. Continuous streamflow data were available from 11 of the sites, and continuous stage data were available from the other 8 sites. High-water mark and discharge-measurement data also were available for model development and testing.

LiDAR data with a vertical accuracy of about 20 cm were processed to produce topographic data for the inundation maps. Bare-earth mass point LiDAR data received from the FMP were reprocessed into a digital elevation model (DEM) with regularly spaced, 1.5-m by 1.5-m cells. A tool was developed as part of this project to connect flow paths (or streams) that were inappropriately disconnected in the DEM by such features as a bridge or road crossing. This process is known as hydroconditioning.

The HEC–RAS model was used for hydraulic modeling. Eleven individual hydraulic models were developed for the Tar River basin sites. Seven models were developed for reaches with a single gage, and four models were developed for reaches of the Tar River main stem that receive flow from major gaged tributaries, or reaches in which multiple gages are near one another. Bathymetric and topographic data used to develop the inundation models were derived from the existing FMP models, LiDAR data, field surveys, and interpolation of measured data.

Overbank cross sections for use in HEC–RAS generally are approximately perpendicular to the stream at the point the cross section intersects the stream, and each cross section intersects the main channel only once. In addition, two cross-section lines cannot intersect each other. Many of the streams in the study area are quite sinuous, so great care was required to develop overbank cross sections that met these requirements. Even so, there were cases, such as near the confluence of a tributary with the main channel, that it was not possible for the overbank cross section to be perpendicular to both the main channel and the tributary. Although overbank cross-section locations were delineated manually for this study, the process has since been automated.

Combined, the Tar River hydraulic models included 272 km of streams in the basin, including about 162 km on the Tar River main stem. Cross-section density in the models was about one cross section per 400 m of stream length, with generally higher densities on tributary streams than on the main stem. The models also included the effects of 59 bridges on flow in the basin.

The hydraulic models were calibrated to the most current stage-discharge relations at 11 long-term streamgages where rating curves were available. Medium- to high-flow discharge measurements were made at some of the sites without rating curves, and high-water marks from Hurricanes Fran and Floyd flooding were available for high-stage calibration. Simulated rating curves matched measured curves over the full range of flows. Differences between measured and simulated water levels for a specified flow were no more than 0.44 m and typically were less. Differences between measured and simulated water levels for models calibrated to high-water marks were less than 0.25 m. These results demonstrate that the 11 Tar River models are capable of simulating accurate water levels over a wide range of steady flows in the Tar River and tributary streams.

The calibrated models were used to generate a set of water-surface profiles for each of the 11 modeled reaches. The profiles were generated at 0.305-m increments for water levels ranging from bankfull to approximately the highest recorded water level at the downstream-most gage in each modeled reach. Inundated areas were identified by subtracting the water-surface elevation in each 1.5-m by 1.5-m grid cell from the land-surface elevation in the cell. An application was developed to identify all inundated cells that were hydraulically connected to the cell at the downstream-most gage in the model domain. All other inundated cells were deleted from the

map layer. This entire process was to create 11 sets of inundation-map libraries for the Tar River basin.

Low-resolution inundation maps that include transportation networks and orthoimagery are accessible on the Internet through the USGS North Carolina Water Science Center's website. These maps also are linked to the USGS National Water Information System website. Hence, a user can determine the near real-time stage and water-surface elevation at a USGS streamgage site in the Tar River basin and link directly to the flood-inundation maps to obtain a depiction of the estimated inundated area at the current water level.

Although the flood-inundation maps represent the boundaries of inundated areas with a distinct line, there is some uncertainty associated with these maps. There are a number of methods for estimating uncertainties associated with hydraulic modeling and inundation mapping, but data required to apply these methods are seldom available, which is true in this case. Flood-inundation models require at least three types of data, all of which contribute to model uncertainty. These are (1) topographic data for the hydraulic model computational grid and the inundation maps, (2) effective friction values (Manning's *n*) for each computational segment (one-dimensional model) or cell (two-dimensional model), and (3) model-validation data of some type. Uncertainties exist in each of these data types. Models applied in near real-time also require a forecast hydrograph.

Land-surface elevation, or topography, is the dominant influence on the location of the simulated shoreline of the inundated area. Results of other studies have demonstrated that low-resolution one-dimensional hydraulic modeling combined with high-resolution topographic data provide good representation of shoreline, which is the reason the original LiDAR data were reprocessed to provide 1.5-m horizontal resolution topographic data in this study.

The HEC–RAS model, which was used in this study, can be adequately calibrated at a point by using a time series of stage and discharge. The model, however, is used to simulate inundation area, so calibration at a single point is not really an adequate calibration, but adequate calibration data are seldom available for inundation models. In addition, streamgage data can be in error by as much as 20 percent or more during extreme floods; thus, improved methods for monitoring floodflows also are needed. An ideal data set for flood-inundation model calibration and validation would include spatially detailed data on the inundation shoreline and, if the models were used to provide estimates of inundation depth, data on water depth throughout the model domain. Several remote-sensing techniques have been used with mixed success in other studies to provide detailed inundation data.

The Tar River flood-inundation maps were developed by using a steady-flow hydraulic model. Two floods at a given location having the same peak flow could have distinctly different inundation patterns. A flood in which water levels rise slowly to the peak and then fall slowly likely will result in more inundation than a flood having the same peak flow but water levels that rise and fall quickly. Simulations using the Tarboro model and the Hurricane Floyd data at Tarboro demonstrated that flows of distinctly different magnitudes can occur for a given water level. According to the model simulations, the inundated areas for the two occurrences of a water-surface elevation of 13.7 m at Tarboro differed by more than 70,000 m^2. These limitations associated with the steady-flow assumption for hydraulic modeling vary from site to site.

The alternative to using the steady-flow assumption and developing inundation-map libraries, as was done for this study, is to estimate inundated areas in real time during or immediately prior to a flood so that particular characteristics of the rainfall and flood hydrograph are well represented in the hydraulic modeling. Results of research studies have demonstrated that this approach is feasible. The limitations of this approach are that the models must be operating in real time for each event, and results must be distributed quickly to emergency management officials and all other interested parties. Moreover, there will be some uncertainty in the forecast flows to the reach for which inundation modeling is to be conducted. The infrastructure and funding for such a system are not in place for the Tar River basin or currently for most locations in the United States. Further studies are needed to investigate the benefits of the real-time system and the map-library approach and to demonstrate the conditions for which each approach is most applicable.

The one-dimensional modeling approach used in this study resulted in good agreement between measured and simulated stage-discharge ratings. One-dimensional hydraulic models, however, are based on the assumption that the hydraulic variables are uniform across a transect. This assumption is reasonable for a prismatic channel in a relatively narrow floodplain but may not be appropriate in broad floodplains for sinuous rivers with several tributaries. Uncertainty in the flood-inundation polygons increases with distance from the main channel for which water-surface slopes are simulated. Two-dimensional models increasingly are used for simulation of floodplain inundation because of the variability in topography across the floodplain, particularly in wide floodplains with numerous tributaries.

References

Bales, J.D., 2003, Effects of Hurricane Floyd inland flooding, September–October 1999, on tributaries to Pamlico Sound, North Carolina: Estuaries, v. 26, no. 5, p. 1319–1328.

Bales, J.D., and Childress, C.J.O., 1996, Aftermath of Hurricane Fran in North Carolina—Preliminary data on flooding and water quality: U.S. Geological Survey Open-File Report 96–499, 6 p.

Bales, J.D., Oblinger, C.J., and Sallenger, A.H., Jr., 2000, Two months of flooding in eastern North Carolina, September–October 1999—Hydrologic, water quality, and geologic effects of Hurricanes Dennis, Floyd, and Irene: U.S. Geological Survey Water-Resources Investigations Report 00–4093, 47 p.

Bates, P.D., 2004, Remote sensing and flood inundation modelling: Hydrological Processes, v. 18, p. 2593–2597.

Bates, P.D., and De Roo, A.P.J., 2000, A simple raster based model for flood inundation simulation: Journal of Hydrology, v. 236, p. 54–77.

Bates, P.D., Wilson, M.D., Horritt, M.S., Mason, D.C., Holden, N., and Currie, A., 2006, Reach-scale floodplain inundation dynamics observed using airborne synthetic aperture radar imagery—Data analysis and modelling: Journal of Hydrology, v. 328, p. 306–318.

Beven, Keith, 2006, On undermining the science?: Hydrological Processes, v. 20, p. 3141–3146.

Brown, J.D., and Damery, S.L., 2002, Managing flood risk in the UK; toward an integration of social and technical perspectives: Transactions of the British Institute of Geographers, v. 27, p. 412–426.

Buchanan, T.J., and Somers, W.P., 1982, Stage measurement at gaging stations: Techniques of Water-Resources Investigations of the United States Geological Survey, book 3, chap. A7, 28 p.

Cobby, D.M., Mason, D.C., and Davenport, I.J., 2001, Image processing of airborne scanning laser altimetry data for improved river flood modelling: Journal of Photogrammetry and Remote Sensing, v. 56, p. 121–138.

Eddins, W.H., and Zembrzuski, T.J., 1998, September 10, 1992, Swain County, North Carolina, *in* Perry, C.A., and Combs, L.J., eds., Summary of floods in the United States, January 1992 through September 1993: U.S. Geological Survey Water-Supply Paper 2499, p. 157–159.

Federal Emergency Management Agency, 2000, High water marks and inundation mapping—Hurricane Floyd: Atlanta, GA, CD 3-v. set.

Fort Collins Office of Emergency Management, 2006, Real time flood inundation mapping & notification system project overview, City of Fort Collins, CO; accessed September 11, 2006, at *http://www.ci.fort-collins.co.us/oem/rtfim.php* .

Hesselink, A.W., Stelling, G.S., Kwadijk, J.C.J., and Middelkoop, H., 2003, Inundation of a Dutch river polder, sensitivity analysis of a physically based inundation model using historic data: Water Resources Research, v. 39, no. 9, 17 p.

Horritt, M.S., and Bates, P.D., 2001, Effects of spatial resolution on a raster based model of flood flow: Journal of Hydrology, v. 253, p. 239–249.

Horritt, M.S., and Bates, P.D., 2002, Evaluation of 1D and 2D numerical models for predicting river flood inundation: Journal of Hydrology, v. 268, p. 87–99.

Hydrologic Engineering Center, 1993, UNET, One-dimensional unsteady flow through a full network of open channels, user's manual: Davis, CA, U.S. Army Corps of Engineers.

Hydrologic Engineering Center, 2002, HEC–RAS river analysis system user's manual, version 3.1: Davis, CA, U.S. Army Corps of Engineers Computer Program documentation report 68; accessed August 30, 2006, at *http://www.hec.usace.army.mil/software/hec-ras/hecras-document.html* [variously paged].

Hydrologic Engineering Center, 2006, HEC–RAS 3.1.3, May 2005 release notes; accessed August 30, 2006, at *http://www.hec.usace.army.mil/software/hec-ras/documents/HEC-RAS3.1.3_Release%20Notes.pdf* .

Islam, M.M., and Sado, Kimiteru, 2002, Development priority map for flood countermeasures by remote sensing data with geographic information system: Journal of Hydrologic Engineering, v. 7, no. 5, p. 346–355.

Jones, J.L., Fulford, J.M., and Voss, F.D., 2002, Near-real-time simulation and internet-based delivery of forecast-flood inundation maps using two-dimensional hydraulic modeling—A pilot study for the Snoqualmie River, Washington: U.S. Geological Survey Water-Resources Investigations Report 2002–4251, 40 p.

Kelly, B.P., and Rydlund, P.H., 2006, Estimated flood-inundation mapping for the lower Blue River in Kansas City, Missouri, 2003–2005: U.S. Geological Survey Scientific Investigations Report 2006–5089; accessed September 11, 2006, at *http://pubs.usgs.gov/sir/2006/5089/* .

Kennedy, E.J, 1990, Levels at streamflow gaging stations: Techniques of Water-Resources Investigations of the United States Geological Survey, book 3, chap. A19, 27 p.

Mason, R.R., Jr., and Caldwell, W.S., 1993, The storm and flood of September 15, 1989, in Fayetteville, North Carolina: U.S. Geological Survey Water-Resources Investigations Report 92–4097, 26 p.

Mason, R.R., Jr., and Jackson, N.M., Jr., 1986, North Carolina surface-water resources, *in* Moody, D.W., Chase, E.B., and Aronson, D.A., eds., National water summary 1985—Hydrologic events and surface-water resources: U.S. Geological Water-Supply Paper 2300, p. 355–360.

Morlock, S.E., Nguyen, H.T., and Ross, J.H., 2002, Feasibility of acoustic Doppler velocity meters for production of discharge records from U.S. Geological Survey streamflow-gaging stations: U.S. Geological Survey Water-Resources Investigations Report 01–4157, 56 p.

National Oceanic and Atmospheric Administration, 2006, Historical hurricane tracks: Coastal Services Center; accessed August 28, 2006, at *http://maps.csc.noaa.gov/hurricanes/viewer.html* .

National Weather Service, 2006, [AHPS] Advance hydrologic prediction service—North Carolina river conditions and forecasts: National Weather Service Southeast River forecast Center; accessed August 28, 2006, at *http://www.srh.noaa.gov/alr/ahps/test1_RVFNC.htm* .

North Carolina Department of Transportation, 2006, Geographic information systems, GIS DOT data (Shapefiles); accessed September 13, 2006, at *http://www.ncdot.org/it/gis/DataDistribution/DOTData/default.html* .

North Carolina Division of Water Quality, 2004, 2004 Tar-Pamlico River basinwide water quality plan, Raleigh, NC; accessed August 25, 2006, at *http://h2o.ehnr.state.nc.us/basinwide/tarpam_draft_dec2003.html* .

North Carolina Floodplain Mapping Program, 2003, LIDAR and digital elevation data fact sheet, Raleigh, NC, North Carolina Floodplain Mapping Program; accessed August 23, 2006, at *http://www.ncfloodmaps.com/pubdocs/lidar_final_jan03.pdf* .

North Carolina Floodplain Mapping Program, 2006, About the North Carolina Floodplain Mapping Program; accessed August 22, 2006, at *http://www.ncfloodmaps.com/pubdocs/NCFPMPHndOut.htm* .

North Carolina Geodetic Survey, 2002, LIDAR quality control status page, QA/QC survey status map, December 31, 2002; accessed August 23, 2006, at *http://www.ncgs.state.nc.us/flood/qc_reports/qc_status.htm* .

Oberg, K.A., Morlock, S.E., and Caldwell, W.S., 2005, Quality-assurance plan for discharge measurements using acoustic Doppler current profilers: U.S. Geological Survey Scientific Investigations Report 2005–5183, 35 p.

Overton, I.C., 2005, Modelling floodplain inundation on a regulated river—Integrating GIS, remote sensing and hydrological models: River Research and Applications, v. 21, p. 991–1001.

Pappenberger, Florian, Beven, K.J., Horritt, M., and Blazkova, S., 2005, Uncertainty in the calibration of effective roughness parameters in HEC–RAS using inundation and downstream water level observations: Journal of Hydrology, v. 302, p. 46–69.

Pappenberger, Florian, Beven, K.J., Hunter, N.M., Bates, P.D., Gouweleeuw, B.T., Thielen, J., and De Roo, A.P.J., 2005, Cascading model uncertainty from medium range weather forecasts (10 days) through a rainfall-runoff model to flood inundation predictions within the European Flood Forecasting System (EFFS): Hydrology and Earth System Sciences, v. 9, no. 4, p. 381–393.

Pielke, R.A., Jr., Downton, M.W., and Barnard Miller, J.Z., 2002, Flood damage in the United States, 1926–2000: A reanalysis of National Weather Service estimates: Boulder, CO, University Corporation for Atmospheric Research, 86 p.; accessed August 23, 2006, at *http://www.flooddamagedata.org/full_report.html* .

Pope, B.F., Tasker, G.D., and Robbins, J.C., 2001, Estimating the magnitude and frequency of floods in rural basins of North Carolina—Revised: U.S. Geological Survey Water-Resources Investigations Report 01–4207, 49 p.

Puech, C., and Raclot, D., 2002, Using geographical information systems and aerial photographs to determine water levels during floods: Hydrological Processes, v. 16, p. 1593–1602.

Rantz, S.E., and others, 1982, Measurement and computation of streamflow: U.S. Geological Survey Water-Supply Paper 2175, 631 p.

Robinson, J.B., Hazell, W.F., and Young, W.S., 1998, Effects of August 1995 and July 1997 storms in the city of Charlotte and Mecklenburg County, North Carolina: U.S. Geological Survey Fact Sheet FS–036–98, 6 p.

Simpson, M.R., 2002, Discharge measurements using a broadband acoustic Doppler current profiler: U.S. Geological Survey Open-File Report 01–01, 123 p.

State Climate Office of North Carolina, 2006, NC Climate Retrieval and Observations Network of the Southeast (NCCRONOS) Database; accessed August 23, 2006, at *http://www.nc-climate.ncsu.edu/cronos/* .

Townsend, P.A., 2001, Mapping seasonal flooding in forested wetlands using multi-temporal Radarsat SAR: Photogrammetric Engineering and Remote Sensing, v. 67, no. 7, p. 857–864.

Toyra, Jessika, Pietroniro, Alain, Martz, L.W., and Prowse, T.D., 2002, A multi-sensor approach to wetland flood monitoring: Hydrological Processes, v. 16, no. 8, p. 1569–1581.

University Corporation for Atmospheric Research, 2006, National data set for flood damage in the United States, 1926–2003, A reanalysis of National Weather Service estimates; accessed August 23, 2006, at *http://www.flooddamagedata.org/national.html* .

U.S. Army Corps of Engineers, 1997, Hurricane Fran—High water marks and inundation mapping: Wilmington, NC [variously paged].

U.S. Census Bureau, 2006a, State & county quick facts—Greenville (city), North Carolina; accessed August 25, 2006, at *http://quickfacts.census.gov/qfd/states/37/3728080.html* .

U.S. Census Bureau, 2006b, State & county quick facts—Rocky Mount (city), North Carolina; accessed August 25, 2006, at *http://quickfacts.census.gov/qfd/states/37/3757500.html* .

U.S. Geological Survey, 2006a, Digital orthophoto quadrangles (DOQs); accessed September 13, 2006, at *http://edcwww.cr.usgs.gov/products/aerial/doq.html* .

U.S. Geological Survey, 2006b, National Water Information System—USGS 02081500 Tar River near Tar River, NC; accessed September 13, 2006, at *http://waterdata.usgs.gov/nc/nwis/uv/?site_no=02081500&PARAmeter_cd=00065,00060* .

U.S. Geological Survey, 2006c, Tar River basin flood-inundation mapping; accessed September 13, 2006, at *http://nc.water.usgs.gov/finmap/index.html* .

U.S. Geological Survey, 2006d, USGS continues to analyze flooding effects from Hurricanes Frances and Ivan in western North Carolina, 2004: U.S. Geological Survey news release; accessed August 22, 2006, at *http://nc.water.usgs.gov/info/news_release/floods04.html* .

Wang, Y., Colby, J.D., and Mulcahy, K.A., 2002, An efficient method for mapping flood extent in a coastal floodplain using Landsat TM and DEM data: International Journal of Remote Sensing, v. 23, no. 18, p. 3681–3696.

Whiteaker, T.L., Robayo, O., Maidment, D.R., and Obenour, D., 2006, From a NEXRAD rainfall map to a flood inundation map: Journal of Hydrologic Engineering, v. 11, no. 1, p. 37–45.

Zembrzuski, T.J., Hill, C.L., Weaver, J.C., Coble, R.W., Gunter, H.C., and Davis, J.M., 1991, North Carolina floods and droughts, *in* Paulson, R.W., Chase, E.B., Roberts, R.S., and Moody, D.W., eds., National water summary 1988–89—Floods and droughts: U.S. Geological Survey Water-Supply Paper 2375, p. 425–434.

Appendix

Example of metadata for the flood-inundation maps.

Identification_Information:
Citation:
Citation_Information:
Originator: Jerad Bales
Originator: Kirsten Cassingham
Publication_Date: Unpublished Material
Title: Flood Inundation area of US Geological Survey Tar River near Tar River; 02081500
Geospatial_Data_Presentation_Form: vector digital data
Online_Linkage:
Description:
Abstract:
Flood inundation maps were created for selected streamgage sites in the Tar River basin, North Carolina. LiDAR data from the North Carolina Floodplain Mapping Program's Floodplain Mapping Information System, available in 10,000-foot by 10,000-foot tiles, were processed to produce topographic data for the inundation maps. Based on root mean square errors between LiDAR data and ground surveys, vertical accuracy of the LiDAR data was about 20 cm. Bare earth mass point LiDAR re-processed into a digital elevation model with regularly spaced, 1.5-meter) by 1.5-meter cells. A tool was developed as part of this project to connect flow paths (or streams) that were inappropriately disconnected in the digital elevation model by some feature such as a bridge or road crossing.

The HEC-RAS model was used for hydraulic modeling at each of the study sites. Eleven individual hydraulic models were developed for the Tar River basin sites. Seven models were developed for reaches with a single gage, and four models were developed for reaches of the Tar River mainstem that receive flow from major gaged tributaries, or reaches in which there were multiple gages near one another.

Combined, the Tar River hydraulic models included 272 kilometers of streams in the basin, including about 162 kilometers on the Tar River mainstem. Cross-section density in the models was about one cross section per 400 meters of stream length, and the models included the effects of 59 bridges on flow in the basin.

The hydraulic models were calibrated to the most current stage-discharge relationship at eleven long-term streamgages where rating curves were available. Medium to high-flow discharge measurements were made at some of the sites without rating curves, and high-water marks from Hurricanes Fran and Floyd were available for high stage calibration. Simulated rating curves matched measured curves over the full range of flows. Differences between measured and simulated water levels for a specified flow were no more than 0.44 m, and typically less.

The calibrated models were used to generate a set of water-surface profiles for each of the 11 modeled reaches at 0.305-meter increments for water levels ranging from bankfull to approximately the highest recorded water level at the downstream-most gage in the each modeled reach. Inundated areas were identified by subtracting the water-surface elevation in each 1.6-meter by 1.6-meter grid cell from the land-surface elevation in the cell through an application that was developed to identify all inundated cells hydraulically connected to the cell at the downstream-most gage in the model domain.

Although the flood inundation maps represent the boundaries of inundated areas with a distinct line on a map, there is some uncertainty associated with these maps. These are uncertainties in topographic data for the hydraulic model computational grid and the inundation maps, effective friction values (Manning's n), model validation data of some type, and forecast hydrographs, if used.

The Tar River flood inundation maps were developed by using a steady-flow hydraulic model. This assumption clearly has less of an effect on inundation maps produced for lower flows than for higher flows because more time typically is required to inundate areas at high flows than at low flows. A flood for which water levels rise slowly to the peak, and then fall slowly will most likely result in more inundation than a flood with the same peak flow, but which rises and falls very quickly. Limitations associated with the steady-flow assumption for hydraulic modeling will vary from site to site.

The one-dimensional modeling approach used in this study resulted in good agreement between measurements and simulations. The one-dimensional approach is reasonable for a prismatic channel in a relatively narrow floodplain, but may not be appropriate in broad floodplains for sinuous rivers with several tributaries. Uncertainty in the flood inundation polygons increases with distance from the main channel for which water-surface slopes were simulated. Two-dimensional models are finding increasing use for simulation of floodplain inundation because of the variability in topography across the floodplain, particularly in wide floodplains with numerous tributaries.

Purpose:

The existing flood information and flood forecasting system has served the State of North Carolina and the Nation well. However, as indicated by experiences during Hurricanes Fran and Floyd, as well as other flood events across the State and Nation, there is a growing demand and need for more and better flood information and flood forecasts. The objective of this project is to develop an enhanced capability for (1) providing flood and flood-related information to emergency managers and the public and (2) producing flood forecasts. The initial phase of the project is focused on the Tar River Basin. The procedures and technology developed in this demonstration study will then be applied throughout the State.

The primary goal of the project is to provide more accessible, informative, timely, and accurate flood information and flood forecast products and for more locations. The project will focus on six specific themes:

- Risk Assessment
- Improved Weather Information
- Real-Time Flood Information and Inundation Mapping
- Enhanced Flood Forecasting
- Flood Forecast Mapping
- Information Delivery System-Integration with NC FMP Information Technology System

Key elements of this project are consistent with those proposed nationally under the NWS AHPS program and the USGS National Streamflow Information Program, as well as the North Carolina Floodplain Mapping Program. This project will ensure that the necessary flood information and forecast capabilities are available in the very near future for North Carolina.

Supplemental_Information:

Eighteen USGS streamgages located in the Tar River Basin were chosen;

02081500	Tar River nr Tar River
02081747	Tar River at US 401 ner Louisburg
02082506	Tar River below Tar River Reservoir ner Rocky Mount
0208250885	Tar River at US 301 Bypass ner Rocky Mount
02082576	Stony Creek at Winstead Ave. at Rock mt
02082585	Tar River at NC97 at Rocky Mount
02082770	Swift Creek at Hilliardston
020828117	Little Fishing Creek nr White Oak
02082950	Fishing Creek nr Enfield
02083000	Fishing Creek at NC97
020833107	Tar River at Tarboro
02083500	Town Creek at US258 nr Pinetops
02083640	Conetoe Creek nr Bethel
02083893	Tar River at US264 Bypass near Greenville
02084000	Tar River at Greenville
02084160	Chcod Creek nr Simpson
02084173	Tar River at SR 1565 nr Grimesland
020873619	Tranters Creek at SR1567 nr Washington

Gages that were in appropriate hydrologic proximity were combined for continuous modeling.

PROCESSING STEPS:

The eighteen gages were processed using Arc Macro Language (aml) programs. They were used to automate and document the steps for further processing of other sites and review. Below are the general steps to produce inundation layers at half foot increments.

1. Locate the XY coordinates for the gage on your line work. Distances from the latitude and longitude were provided by the Hydrologic Engineering Centers River Analysis System (HEC-RAS) model. Each point is a measured distance from the gage with an associated elevation of inundation at half foot increments.

2. A line coverage is then digitized perpendicular to the stream which also crosses the points of elevation. These arcs are then used to interpolate inundated surfaces using TOPOGRID (contour, xyzlimits).

3. A "depth" grid is generated by subtraction of the surface (inundated surfaces at half increments) from the digital elevation model. This grid provides a grid of water depth above sea level.

4. REGIONGROUP was used to select the connecting cells on 4 sides. This grid is used as a mask to give the "depth" grid lateral definition.

5. Grids at each inundation level are then merged to one grid. This grid is then converted to a polygon coverage or shapefile. The values of inundated elevations and depths are then joined to the associated table.

DISCLAIMER:

Any use of trade, product, or firm names is for descriptive purposes only and does not imply endorsement by the U.S. Government. Although this Federal Geographic Data Committee-compliant metadata file is intended to document the data set in nonproprietary form, as well as in ARC/INFO format, this metadata file may include some ARC/INFO-specific terminology.

Time_Period_of_Content:
Time_Period_Information:
Single_Date/Time:
Calendar_Date: unknown
Currentness_Reference: publication date
Status:
Progress: Complete
Maintenance_and_Update_Frequency: None planned
Spatial_Domain:
Bounding_Coordinates:
West_Bounding_Coordinate: -78.649111
East_Bounding_Coordinate: -78.569046
North_Bounding_Coordinate: 36.228350
South_Bounding_Coordinate: 36.168764
Keywords:
Theme:
Theme_Keyword_Thesaurus: None
Theme_Keyword: Flood
Theme_Keyword: Inundation
Theme_Keyword: floodzones
Theme_Keyword: LIdar derived
Place:
Place_Keyword_Thesaurus: None
Place_Keyword: US
Place_Keyword: North Carolina
Place_Keyword: Tar River Basin
Place_Keyword: Rocky Mount
Access_Constraints:
Any use of trade, product, or firm names is for descriptive purposes only and does not imply endorsement by the U.S. Government.

Although this Federal Geographic Data Committee-compliant metadata file is intended to document the data set in nonproprietary form, as well as in ARC/INFO format, this metadata file may include some ARC/INFO-specific terminology.

Use_Constraints:
Any use of trade, product, or firm names is for descriptive purposes only and does not imply endorsement by the U.S. Government.

Although this Federal Geographic Data Committee-compliant metadata file is intended to document the data set in nonproprietary form, as well as in ARC/INFO format, this metadata file may include some ARC/INFO-specific terminology.

Point_of_Contact:
Contact_Information:
Contact_Person_Primary:
Contact_Person: Jerad Bales

Contact_Organization: USGS
Contact_Position: Hydrologist
Contact_Voice_Telephone: 919-571-4000
Contact_Facsimile_Telephone: 919-5714041
Native_Data_Set_Environment: Microsoft Windows XP Version 5.1 (Build 2600) Service Pack 2; ESRI ArcCatalog 9.0.0.535
Data_Quality_Information:
Lineage:
Process_Step:
Process_Description: Metadata imported.
Process_Step:
Process_Description: Metadata imported.
Source_Used_Citation_Abbreviation: C:\DOCUME~1\kmcassin\LOCALS~1\Temp\xml4C2E.tmp
Process_Step:
Process_Description: Metadata imported.
Source_Used_Citation_Abbreviation: C:\DOCUME~1\kmcassin\LOCALS~1\Temp\xml25B4.tmp
Process_Step:
Process_Description: Dataset copied.
Source_Used_Citation_Abbreviation: I:\tarriver_tarriver\cf-grids\fl1500
Spatial_Data_Organization_Information:
Direct_Spatial_Reference_Method: Vector
Point_and_Vector_Object_Information:
SDTS_Terms_Description:
SDTS_Point_and_Vector_Object_Type: Complete chain
Point_and_Vector_Object_Count: 861239
SDTS_Terms_Description:
SDTS_Point_and_Vector_Object_Type: Label point
Point_and_Vector_Object_Count: 386978
SDTS_Terms_Description:
SDTS_Point_and_Vector_Object_Type: GT-polygon composed of chains
Point_and_Vector_Object_Count: 386978
SDTS_Terms_Description:
SDTS_Point_and_Vector_Object_Type: Point
Point_and_Vector_Object_Count: 4
SDTS_Terms_Description:
SDTS_Point_and_Vector_Object_Type: Composite object
Point_and_Vector_Object_Count: 51
Spatial_Reference_Information:
Horizontal_Coordinate_System_Definition:
Planar:
Map_Projection:
Map_Projection_Name: Lambert Conformal Conic
Lambert_Conformal_Conic:
Standard_Parallel: 34.333333
Standard_Parallel: 36.166667
Longitude_of_Central_Meridian: -79.000000
Latitude_of_Projection_Origin: 33.750000
False_Easting: 2000000.002617
False_Northing: 0.000000
Planar_Coordinate_Information:
Planar_Coordinate_Encoding_Method: coordinate pair
Coordinate_Representation:
Abscissa_Resolution: 0.000064

Ordinate_Resolution: 0.000064
Planar_Distance_Units: survey feet
Geodetic_Model:
Horizontal_Datum_Name: North American Datum of 1983
Ellipsoid_Name: Geodetic Reference System 80
Semi-major_Axis: 6378137.000000
Denominator_of_Flattening_Ratio: 298.257222
Entity_and_Attribute_Information:
Detailed_Description:
Entity_Type:
Entity_Type_Label: fl1500.pat
Entity_Type_Definition: Regions dissolved into grid-code values
Attribute:
Attribute_Label: FID
Attribute_Definition: Internal feature number.
Attribute_Definition_Source: ESRI
Attribute_Domain_Values:
Unrepresentable_Domain: Sequential unique whole numbers that are automatically generated.
Attribute:
Attribute_Label: Shape
Attribute_Definition: Feature geometry.
Attribute_Definition_Source: ESRI
Attribute_Domain_Values:
Unrepresentable_Domain: Coordinates defining the features.
Attribute:
Attribute_Label: AREA
Attribute_Definition: Area of feature in internal units squared.
Attribute_Definition_Source: ESRI
Attribute_Domain_Values:
Unrepresentable_Domain: Positive real numbers that are automatically generated.
Attribute:
Attribute_Label: PERIMETER
Attribute_Definition: Perimeter of feature in internal units.
Attribute_Definition_Source: ESRI
Attribute_Domain_Values:
Unrepresentable_Domain: Positive real numbers that are automatically generated.
Attribute:
Attribute_Label: FL1500#
Attribute_Definition: Internal feature number.
Attribute_Definition_Source: ESRI
Attribute_Domain_Values:
Unrepresentable_Domain: Sequential unique whole numbers that are automatically generated.
Attribute:
Attribute_Label: FL1500-ID
Attribute_Definition: User-defined feature number.
Attribute_Definition_Source: ESRI
Attribute:
Attribute_Label: GRID-CODE
Attribute_Definition: Each number starting with 1 represents half foot increments in flooding areas.
Attribute:
Attribute_Label: ELEV-MSL
Attribute_Definition: Elevation at mean sea level.

Attribute:
Attribute_Label: SURF-RANGE
Attribute_Definition: Range at half foot values of surface water at mean sea level.
Attribute:
Attribute:
Detailed_Description:
Entity_Type:
Entity_Type_Label: fl1500.patsub
Entity_Type_Definition: Attribute table
Attribute:
Attribute_Label: FID
Attribute_Definition: Internal feature number.
Attribute_Definition_Source: ESRI
Attribute_Domain_Values:
Unrepresentable_Domain: Sequential unique whole numbers that are automatically generated.
Attribute:
Attribute_Label: Shape
Attribute_Definition: Feature geometry.
Attribute_Definition_Source: ESRI
Attribute_Domain_Values:
Unrepresentable_Domain: Coordinates defining the features.
Attribute:
Attribute_Label: AREA
Attribute_Definition: Area of feature in internal units squared.
Attribute_Definition_Source: ESRI
Attribute_Domain_Values:
Unrepresentable_Domain: Positive real numbers that are automatically generated.
Attribute:
Attribute_Label: PERIMETER
Attribute_Definition: Perimeter of feature in internal units.
Attribute_Definition_Source: ESRI
Attribute_Domain_Values:
Unrepresentable_Domain: Positive real numbers that are automatically generated.
Attribute:
Attribute_Label: SUB#
Attribute_Definition: Internal feature number.
Attribute_Definition_Source: ESRI
Attribute_Domain_Values:
Unrepresentable_Domain: Sequential unique whole numbers that are automatically generated.
Attribute:
Attribute_Label: SUB-ID
Attribute_Definition: User-defined feature number.
Attribute_Definition_Source: ESRI
Attribute:
Attribute_Label: GRID-CODE
Distribution_Information:
Resource_Description: Downloadable Data
Standard_Order_Process:
Digital_Form:
Digital_Transfer_Information:
Transfer_Size: 202.097

Metadata_Reference_Information:
  Metadata_Date: 20061027
  Metadata_Contact:
    Contact_Information:
      Contact_Organization_Primary:
        Contact_Organization: US Geological Survey, WRD
        Contact_Person: Kirsten C. Tighe
      Contact_Address:
        Address_Type: mailing and physical address
        Address: 3916 Sunset Ridge Rd.
        City: Raleigh
        State_or_Province: North Carolina
        Postal_Code: 27609
      Contact_Voice_Telephone: 919-571-4050
      Contact_Facsimile_Telephone: 919-571-4041
  Metadata_Standard_Name: FGDC Content Standards for Digital Geospatial Metadata
  Metadata_Standard_Version: FGDC-STD-001-1998
  Metadata_Time_Convention: local time
  Metadata_Extensions:
    Online_Linkage: http://www.esri.com/metadata/esriprof80.html
    Profile_Name: ESRI Metadata Profile
  Metadata_Extensions:
    Online_Linkage: http://www.esri.com/metadata/esriprof80.html
    Profile_Name: ESRI Metadata Profile
  Metadata_Extensions:
    Online_Linkage: http://www.esri.com/metadata/esriprof80.html
    Profile_Name: ESRI Metadata Profile
  Metadata_Extensions:
    Online_Linkage: http://www.esri.com/metadata/esriprof80.html
    Profile_Name: ESRI Metadata Profile

Prepared by:
U.S. Geological Survey
Enterprise Publishing Network
Raleigh Publishing Service Center
3916 Sunset Ridge Road
Raleigh, NC 27607

A PDF version of this publication is available online at URL
http://pubs.water.usgs.gov/sir2007–5032/